# Chemoselective Cyclopropanation over Carbene Y—H insertion Catalyzed by an Engineered Carbene Transferase

Eric J. Moore<sup>‡</sup>, Viktoria Steck<sup>‡</sup>, Priyanka Bajaj, and Rudi Fasan\*

Department of Chemistry, University of Rochester, Rochester, New York 14627, United States.

**ABSTRACT:** Hemoproteins have recently emerged as promising biocatalysts for promoting a variety of carbene transfer reactions including cyclopropanation and Y—H insertion (Y = N, S, Si, B). For these and synthetic carbene transfer catalysts alike, achieving high chemoselectivity toward cyclopropanation in olefin substrates bearing unprotected Y—H groups has proven remarkably challenging due to competition from the more facile carbene Y—H insertion reaction. In this report, we describe the development of a novel artificial metalloenzyme based on an engineered myoglobin incorporating a serine-ligated Co-porphyrin cofactor that is capable of offering high selectivity toward olefin cyclopropanation over N—H and Si—H insertion. Intramolecular competition experiments revealed a distinct and dramatically altered chemoselectivity of the Mb(H64V,V68A,H93S)[Co(ppIX)] variant in carbene transfer reactions compared to myoglobin based variants containing the native histidine-ligated heme cofactor or other metal/proximal ligand substitutions. These studies highlight the functional plasticity of myoglobin as a 'carbene transferase' and illustrate how modulation of the cofactor environment within this metalloprotein scaffold represents a valuable strategy for accessing carbene transfer reactivity not exhibited by naturally occurring hemoproteins or transition metal catalysts.

### Introduction

The transition-metal catalyzed insertion of carbenoids into C=C, C-H, and Y—H bonds (Y = N, S, O, Si, B), represents an important class of transformations for the construction of new carbon-carbon and carbon-heteroatom bonds.¹ A plethora of organometallic catalysts, including Rh-, Ir-, Ru-, Cu-, Co-, and Fe-based complexes, have been reported to promote these transformations.¹ More recently, our group and others have demonstrated the ability of engineered hemoproteins derived from myoglobin,² and cytochrome P450s,³, respectively, to provide viable biocatalysts for mediating olefin cyclopropanations as well as other types of carbene-mediated transformations, including N—H insertion,⁴ S—H insertion,⁵ and Si—H insertion.⁶ Artificial 'carbene transferases' based on these²c,७ or other protein scaffolds8 have also been reported.

Among carbene-mediated transformations, olefin cyclopropanations are particularly attractive owing to the relevance of cyclopropane rings as structural motifs in medicinal chemistry and drug discovery. Despite major progress made in transition metal-catalyzed carbene transfer chemistry,1 the development of catalytic systems capable of favoring olefin cyclopropanation over carbene Y—H insertion reactions has remained an unmet challenge. Indeed, studies involving different types of organometallic catalysts invariably showed that the more facile Y—H carbene insertion outcompetes olefin cyclopropanation in both inter- and intramolecular settings.<sup>10</sup> A similar reactivity trend is exhibited by hemoprotein-based carbene transfer catalysts, as documented by our own studies (vide infra) and reports from other groups. 4a,6 Indeed, Arnold and coworkers reported the exclusive occurrence of N—H insertion in the P450-catalyzed transformation of p-amino-styrene with ethyl  $\alpha$ -diazoacetate<sup>4a</sup> and exclusive formation of the Si—H insertion product in the cytochrome c-catalyzed transformation of a silane group-containing styrene derivative with ethyl α-diazopropanoate. In this context, the development of carbene transfer catalysts capable of favoring cyclopropanation in substrates bearing unprotected Y—H groups is highly desirable as these systems would not only complement the chemoselectivity of (bio)catalysts currently available for these reactions, but also disclose new opportunities toward the selective cyclopropanation of densely functionalized olefin substrates. Herein, we report the development and characterization of a myoglobin-based biocatalyst that is able to display high chemoselectivity toward olefin cyclopropanation over N—H and Si—H insertion, a unique reactivity acquired through substitution of the native histidineligated heme cofactor with a non-native serine-ligated Coporphyrin.

### **Results and Discussion**

At the incipit of these studies, we selected the Mb(H64V,V68A) variant as the starting point for catalyst development in reason of its high catalytic activity (>10,000 turnovers (TON)) and stereoselectivity (95-99% de and ee) in the cyclopropanation of vinylarene substrates in the presence of ethyl α-diazoacetate (EDA) as the carbene donor.2a This variant also exhibits high activity toward the functionalization of arylamines4b and mercaptan substrates<sup>5</sup> with diazoester reagents via carbene N—H and S— H insertion, respectively. Carbene insertion into the Si—H bonds of silanes is a facile transformation for carbene transfer catalysts.11 To assess the Si-H insertion activity of Mb(H64V,V68A), we examined the transformation of dimethylphenyl silane (1a) in presence of EDA (2) to give the functionalized product 1b (Table 1). As expected, this reaction proceeded efficiently resulting in the clean formation of the Si—H insertion product in 66% yield in the presence of 0.2 mol% catalyst (330 TON; Table 1, Entry 3). By comparison, negligible Si—H insertion activity was observed for free hemin (15 TON; **Table 1**, Entry 1), whereas wild-type sperm whale myoglobin (Mb) displayed a two-fold lower activity compared to the Mb(H64V,V68A) variant (175 TON; Table 1, Entry 2). Under catalyst-limited conditions, Mb(H64V,V68A) was found to support over 1,500 turnovers in this reaction (Table 1. Entry 4). This catalytic activity compares favorably with that recently reported for the same silane substrate and ethyl  $\alpha$ -diazopropanoate by an engineered cytochrome c variant optimized by directed evolution for this reaction (2,520 TON)6 or that of other metallopeptide/protein complexes investigated in the context of related Si—H insertion reactions. 12 Altogether, these results demonstrated that Si-H insertion reactions are readily catalyzed by the Mb-based 'carbene transferase', as expected based on its previously observed reactivity toward other electronrich Y—H substrates.4b,5

On the basis of these results, we were interested in assessing the chemoselectivity of Mb(H64V,V68A) in the cyclopropanation of 4-(dimethylsilyl)styrene (3a), in which the silane group (Si—H) can compete for carbene insertion with the olefinic group (Table 2). This reaction led to minimal formation (4%) of the desired cyclopropane product 3b, with the Si—H insertion adduct 3c representing the largely predominant product (96%; Table 2, Entry 2). Albeit with lower efficiency (1-10% vs. 13% conv.), a similar reactivity profile was observed for a variety of other hemoproteins, including horseradish peroxidase (HRP), catalase,

cytochrome P450<sub>BM3</sub> and its engineered variant FL#62<sup>13</sup>, and cytochrome c (**Table 2**, Entries 3-7), with which the cyclopropanation product **3b** is formed only in minor amounts (<5-11%) compared to the Si—H insertion product. The results with wild-type equine heart cytochrome c are consistent with those recently reported in a related reaction with cytochrome c from *Rhodothermus marinus*.6

Table 1. Myoglobin-catalyzed carbene Si—H insertion with dimethylphenyl silane 1a and EDA 2.<sup>a</sup>

Table 2. Chemoselectivity of myoglobin and other hemoproteins in the reaction with 4-(dimethylsilyl)styrene (3a) or *para*-amino-styrene (4a) and EDA.<sup>a</sup>

	2 ( )			` '	
En- try	Catalyst	% yield (3b+3c) <sup>b</sup>	3b:3c ratio	% yield (4b+4c) <sup>b</sup>	4b:4c ratio
1	Mb	6	3:97	65	1:99
2	Mb(H64V,V68A)	13	4:96	85	0:100
3	HRP	1	11:89	96	0:100
4	Catalase	1	9:91	6	2:98
5	P450 <sub>BM3</sub>	<0.5	5:95	24	1:99
6	FL#62	4	5:95	25	1:99
7	cytochrome c	10	5:95	57	1:99

 $<sup>^</sup>a$  Reaction conditions: 10 mM **3a** or **4a**, 10 mM EDA, 10 mM Na<sub>2</sub>S<sub>2</sub>O<sub>4</sub>, 20 μM catalyst in 50 mM phosphate buffer (pH 7.0).  $^b$  Based on GC conversion using calibration curves with isolated **3b**, **3c**, **4b**, and **4c**.

 $<sup>^</sup>a$  Reaction conditions: 10 mM dimethylphenyl silane, 20 mM EDA, 10 mM Na<sub>2</sub>S<sub>2</sub>O<sub>4</sub>, 1-100  $\mu$ M catalyst in 50 mM phosphate buffer (pH 7.0).  $^b$  Based on GC conversion using calibration curves with isolated  ${\bf 1b}.$ 

To examine the relative reactivity toward olefin cyclopropanation vs. N-H insertion, similar experiments were conducted in the presence of para-amino-styrene (4a) and EDA as the carbene donor reagent. Interestingly, in addition to Mb(H64V,V68A), horseradish peroxidase and cytochrome c were found to be particularly active in the transformation of this substrate, leading to the N—H insertion product in 96% and 57% yield, respectively (**Table 2**, Entries 3 and 7). For these and all the other hemoproteins, however, the desired cyclopropanation product 3b was either not formed (HRP) or produced only in negligible amounts (<1-2%). Along with observations previously made with synthetic catalysts, 10a-c these results corroborated the notion that preferential formation of the cyclopropanation product in substrates containing an unprotected Si—H or N—H group is not attainable using currently available carbene transfer catalysts and biocatalysts.

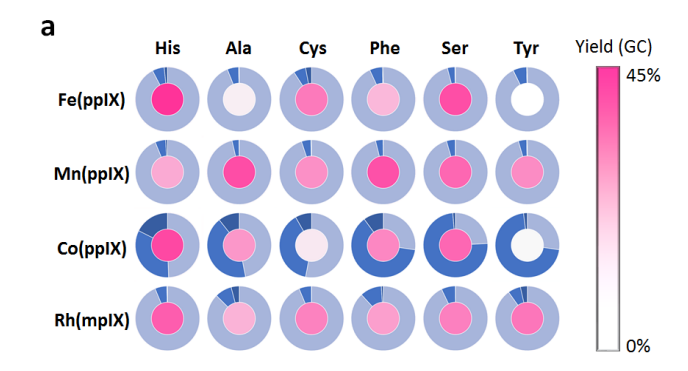
The carbene transfer activity of Mb hinges upon the formation of a carbene-heme intermediate at the level of the active site (i.e., distal heme pocket), <sup>2a</sup> whose reactivity is influenced by the nature of the porphyrin ligand and axial residue.<sup>14</sup> Previously, we established that modification of the metalloporphyrin cofactor environment within this scaffold, i.e., through substitution of the metal, 2c porphyrin ligand,<sup>7a</sup> or metal-ligating proximal residue,<sup>14</sup> can modulate the carbene transfer reactivity of this metalloprotein. Based on these findings, we hypothesized that this approach could furnish a means to tune the chemoselectivity of myoglobinbased cyclopropanation catalysts and thus access Mb variants capable of favoring olefin cyclopropanation over the inherently more facile carbene Y—H insertions in functionalized substrates where both reactions are possible (e.g., 3a and 4a).

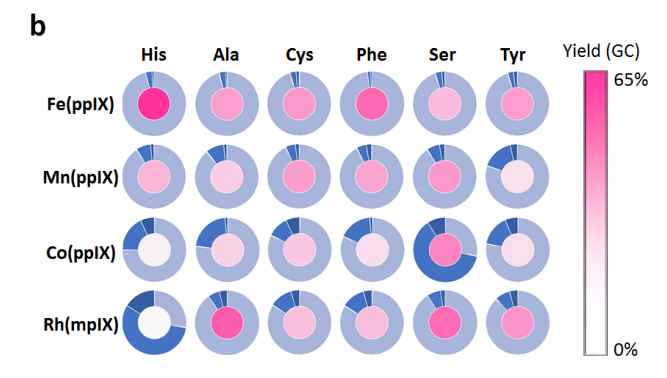
Toward this goal, we prepared a library of Mb(H64V,V68A) derived variants in which the native heme is substituted with Co(ppIX), Mn(ppIX), and Rh(mpIX)). In addition, the native metal-coordinating His residue (His93) was varied to include alternative nucleophilic residues (i.e., Cys, Ser, Tyr) as well as non-Lewis basic amino acids (i.e., Ala and Phe). Based on the available crystal structure of Mb, 15 the His93Ala and His93Phe variants were expected to alter steric access at the proximal side of the metalloporphyrin cofactor for either enabling or disfavoring, respectively, axial coordination of the metal by a water molecule. Conveniently, these artificial metalloenzymes could be produced directly in *E. coli* cells arrayed in 96-well plates by exploiting our recently introduced protocol for the recombinant expression of cofactor-substituted myoglobins. 2c,16

The catalytic activity and selectivity toward cyclopropanation vs. Si—H insertion of the cofactor-modified Mb variants was then assessed in whole-cell reactions<sup>2b</sup> containing 4-(dimethylsilyl)styrene **3a** and EDA. The results from these experiments are graphically summarized in **Figure 1a** and the most representative data are provided in **Table 3**. Interestingly, these analyses revealed a significant impact of both the metal and proximal residues on the catalytic activity and chemoselectivity of the reaction. For example, in the presence of the native heme cofactor (Fe(ppIX)), only the His93Ser variant exhibited comparable activity to the parent protein Mb(H64V,V68A) (**Table 3**, Entries 1 and 2). In contrast, the most active catalysts among the Mn-containing

Mb variants feature a non-nucleophilic residue (i.e., Ala or Phe) in place of the proximal histidine residue (**Table 3**, entries 3-5). More importantly, heme replacement with the non-native cofactor Co-protoporphyrin IX (Co(ppIX)) induced a dramatic shift in the chemoselectivity of the Mb catalyst to favor the formation of the cyclopropanation product, leading to **3b:3c** ratios ranging from 40:60 to 74:26 (**Figure 1a**). This reactivity is in stark contrast with that of the Fe-, Mn-, and Rh-containing variants, which greatly favors the formation of the Si—H insertion product (**3b:3c** ratios from 4:96 to 11:89; **Figure 1a**).

**Figure 1.** Screening data for the cofactor/proximal ligand substituted Mb(H64V,V68A) variants in the reactions with (a) 4-(dimethylsilyl)styrene **3a** or (b) 4-amino-styrene **4a**, and EDA. The pie charts indicate the product distribution (light blue for Si—H and N—H insertion products **3c** and **4c**, respectively; blue for cyclopropanation product **3b** and **4b**, respectively; dark blue for multiple insertion byproduct(s)). The activity (% GC yield) is represented as filling color.





Among the Co-substituted variants, Mb(H64V,V68A,H93S)[Co(ppIX)] displayed the most optimal combination of high chemoselectivity for cyclopropanation over Si—H insertion (74% selectivity) and good catalytic activity (**Table 3**, Entry 7). Attempts to further optimize the Mb(H64V,V68A,H93S)[Co(ppIX)]-catalyzed reaction by varying the substrate loading and/or **3a**: EDA ratio, did not result in significant improvements in the yield of **3b**, indicating that the reaction conditions applied during the catalyst screening were already optimal for this transformation.

From the systematic set of structure-activity data collected in these experiments, it became apparent that whereas the cobalt metal center is critical for inducing the desired selectivity toward cyclopropanation  $(6\%\rightarrow33\%)$ ;

**Table 3**, Entry 6 vs. 1), axial coordination by the serine residue is beneficial toward enhancing this reactivity  $(33\% \rightarrow 74\%;$  **Table 3**, Entry 7 vs. 6). Control experiments using free Co(ppIX) as the catalyst (2 mol%) under identical reaction conditions  $(10 \text{ mM } 3a, 10 \text{ mM EDA}, 10 \text{ mM Na}_2\text{S}_2\text{O}_4$  in phosphate buffer, pH 7.2) resulted in negligible formation of product (<1% yield), most of which consisted of the Si—H insertion product (80%). These results further evidenced the critical role of the protein matrix in modulating the reactivity and selectivity of the Co-protoporphyrin IX cofactor.

Encouraged by these results, the panel Mb(H64V,V68A)-based variants was screened against 4amino-styrene (4a), in which carbene insertion into the N— H bond of the amino group was found to greatly outcompete cyclopropanation of the C=C double bond in the reactions catalyzed by Mb(H64V,V68A) and other carbene transfer (bio)catalysts (Table 2). As shown by the data summarized in **Figure 1b**, also in this case substitution of the metal and axial ligand was found to alter significantly the efficiency and/or chemoselectivity of the reaction. Specifically, all the Fe-containing variants maintain high preference for the N— H insertion reaction (95-96%) over the cyclopropanation reaction, regardless of the nature of the proximal residue. Most of these variants also display significantly reduced activity compared to Mb(H64V,V68A), with the only exception of the H93F variant, whose catalytic activity is only moderately affected (47% vs 63% yield; **Table 4**, Entries 2 vs. 1).

Table 3. Catalytic activity and selectivity of selected Mb(H64V,V68A) variants in the reaction with 4-(dimethylsilyl)styrene (3a) and EDA.<sup>a</sup>

Me Me ODET Mb catalyst (whole cells) 
$$Me - Si$$
  $Me - Si$   $Me - Si$ 

En-	Protein	Cofactor	%	%	%
try			yield <sup>b</sup>	$3b^c$	$3c^{c}$
1	Mb(H64V,V68A)	Fe(ppIX)	41	6	92
2	Mb(H64V,V68A,H93S)	Fe(ppIX)	36	4	96
3	Mb(H64V,V68A)	Mn(ppIX)	18	5	94
4	Mb(H64V,V68A,H93A)	Mn(ppIX)	36	3	96
5	Mb(H64V,V68A,H93F)	Mn(ppIX)	35	4	96
6	Mb(H64V,V68A)	Co(ppIX)	37	33	49
7	Mb(H64V,V68A,H93S)	Co(ppIX)	44	74	24
8	Mb(H64V,V68A,H93F)	Co(ppIX)	25	63	10
9	Mb(H64V,V68A)	Rh(mpIX)	33	6	94

<sup>&</sup>lt;sup>a</sup> Reaction conditions: 10 mM **3a**, 10 mM EDA, *E. coli* whole cells expressing Mb variant (0D $_{600}$  = 40) in 50 mM phosphate buffer (pH 7.2). <sup>b</sup> Based on GC conversion using calibration curves with isolated **3b** and **3c**. <sup>c</sup> The remainder to 100% corresponds to double insertion product(s).

In comparison, metal substitution appeared to have a more profound impact on the chemoselectivity of the metalloprotein catalyst. Across the board, the Co-substituted variants displayed a more pronounced propensity to promote the formation of the cyclopropanation product **4b** (10-62% selectivity; **Figure 1b**) when compared to the Mncontaining variants and most of the Rh-containing variants (5-15% selectivity).

As observed for the Si—H insertion vs. cyclopropanation reaction with **3a**, the Mb variant combining the Co(ppIX) and His93Ser substitution emerged as the most efficient and chemoselective catalyst for promoting the cyclopropanation of **4a** to give the desired product **4b** (62% selectivity: **Table 4**, Entry 7). Again, coordination of the cobalt center by the serine residue appears to be critical for enhancing this chemoselectivity feature, as evidenced by the 3- to 6fold higher selectivity of this variant toward favoring cyclopropanation over N—H insertion when compared to both the histidine-ligated and the structurally similar cysteine-ligated counterparts (Table 4, Entry 7 vs. 5 and 6). The Mb(H64V,V68A,H93S)[Co(ppIX)]-catalyzed conversion of **4a** could be further optimized to yield the cyclopropanation product 4b with 72% selectivity in 45% yield (Table 3, Entry 8). Control reactions with free Co(ppIX) cofactor in buffer show minimal conversion of 4a to a mixture of 4b and 4c (<1% yield).

Table 4. Catalytic activity and selectivity of selected Mb(H64V,V68A) variants in the reaction with 4-aminostyrene (4a) and EDA.<sup>a</sup>

En-	Protein	Cofactor	%	%	%
try			yield <sup>b</sup>	4bc	4cc
1	Mb(H64V,V68A)	Fe(ppIX)	63	3	96
2	Mb(H64V,V68A,H93F)	Fe(ppIX)	47	2	98
3	Mb(H64V,V68A)	Mn(ppIX)	25	7	91
4	Mb(H64V,V68A,H93Y)	Mn(ppIX)	11	16	81
5	Mb(H64V,V68A)	Co(ppIX)	6	18	75
6	Mb(H64V,V68A,H93C)	Co(ppIX)	19	10	83
7	Mb(H64V,V68A,H93S)	Co(ppIX)	38	62	28
8 <sup>d</sup>	Mb(H64V,V68A,H93S)	Co(ppIX)	45	72	24
9	Mb(H64V,V68A)	Rh(mpIX)	4	56	28
10	Mb(H64V,V68A,H93A)	Rh(mpIX)	50	6	90

 $^{\rm a}$  Reaction conditions: 10 mM **4a**, 10 mM EDA, *E. coli* whole cells expressing Mb variants (OD<sub>600</sub> = 40) in 50 mM phosphate buffer (pH 7.2).  $^{\rm b}$  Based on GC conversion using calibration curves with isolated **4b** and **4c**.  $^{\rm c}$  The remainder to 100% corresponds to double insertion product(s).  $^{\rm d}$  With 10 mM **4a**, 7.5 mM EDA, and whole cells at OD<sub>600</sub> = 80.

Interestingly, the Rh-based variant Mb(H64V,V68A)[Rh(mpIX)] also exhibited significantly improved selectivity toward cyclopropanation vs. N—H insertion compared to the parent variant Mb(H64V,V68A)  $(3\% \rightarrow 56\% \text{ selectiv.};$ **Table 4**, Entry 9 vs. 1). However, this change in chemoselectivity is accompanied by a drastic reduction in catalytic activity, making it an inferior catalyst compared to Mb(H64V,V68A,H93S)[Co(ppIX)]. Still, it is interesting to note the distinctive effect of the proximal histidine toward inducing the observed chemoselectivity shift in the Rh-based variant compared to the other residues introduced at this position (Figure 1b) or to the His93Ala counterpart, in which axial coordination of the metal is not avail-(Table 4, Entry 10 VS. 9). Mb(H64V,V68A,H93S)[Co(ppIX)], these results highlight the interplay of the effects resulting from metal and proximal ligand variation in tuning the reactivity and chemoselectivity of these biocatalysts.

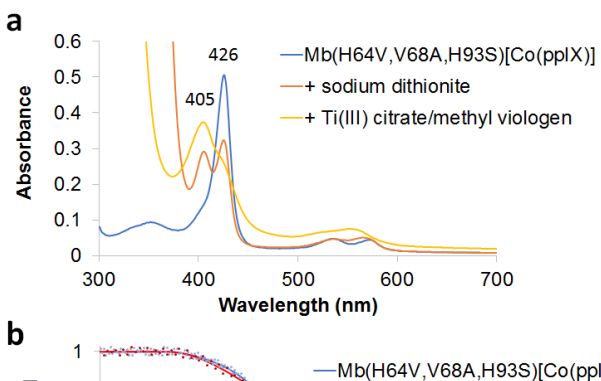
Based results Mb(H64V,V68A,H93S)[Co(ppIX)] was selected for further characterization. This variant could be efficiently expressed and isolated from *E. coli* as holoprotein in good yields (~8 mg/L culture). Its UV-vis spectrum shows a strong absorption band at 425 nm and two weak absorption bands at 535 and 570 nm, corresponding to the Soret and Q-bands of the protein, respectively (Figure 2a). Upon addition of sodium dithionite (Na<sub>2</sub>S<sub>2</sub>O<sub>4</sub>), the Soret band shifts to 405 nm, which was assigned to the reduced, Co(II) form of the metalloprotein. Unlike the iron-based counterpart, only partial reduction (~40%) of Mb(H64V,V68A,H93S)[Co(ppIX)] was observed with excess sodium dithionite even after overnight incubation (Figure 2a, red line). More efficient conversion to the reduced form of this protein was achieved instead using the stronger reductant Ti(III) citrate in combination with the electron transfer mediator methyl viologen (Figure 2a, orange line).17

Control experiments involving reactions with 3a or 4a in the presence of either the oxidized or reduced form of Mb(H64V,V68A,H93S)[Co(ppIX)] revealed that the latter species is catalytically less active but more selective for cyclopropanation over Si—H (or N—H) insertion compared to the oxidized form of the protein. Moreover, both TON and the cyclopropanation vs. Y—H insertion chemoselectivity obtained with the purified protein were lower than those achieved in the whole cell reactions, clearly indicating a favorable effect of the intracellular environment on the catalytic performance of this biocatalyst. This effect can be in attributed to the efficient reduction Mb(H64V,V68A,H93S)[Co(ppIX)] within the reducing intracellular milieu, as suggested by UV-vis spectroscopy analysis of cell lysates (Co(II):Co(III) > 9:1). Through thermal denaturation experiments using circular dichroism (CD), we further determined Mb(H64V,V68A,H93S)[Co(ppIX)] variant has an apparent melting temperature ( $T_m$ ) of 60.0°C ± 0.2 (**Figure 2b**). This  $T_m$  value is comparable to that of Mb(H64V,V68A) (66.0°C ± 1.0), 18 indicating that remodeling of the cofactor environment in this variant did not significantly affect the stability of the metalloprotein.

To gain further insights into the chemoselectivity properties of Mb(H64V,V68A,H93S)[Co(ppIX)], this and other

selected variants were tested in an intramolecular competition experiment using 4-(dimethylsilyl)aniline **5a**, in which N–H insertion competes for Si–H insertion (**Table 5**). These studies showed that Mb(H64V,V68A,H93S)[Co(ppIX)] exhibits a strong preference toward the N—H insertion

**Figure 2.** Characterization of Mb(H64V,V68A,H93S)-[Co(ppIX)]. (a) Overlay of the electronic absorption spectra of the protein prior to (blue) and after reduction with sodium dithionite (red) or Ti(III) citrate (orange). (b) Thermal denaturation curves for Mb(H64V,V68A) (green) and Mb(H64V,V68A,H93S)[Co(ppIX)] (red) as determined by circular dichroism ( $\theta_{222}$ ).



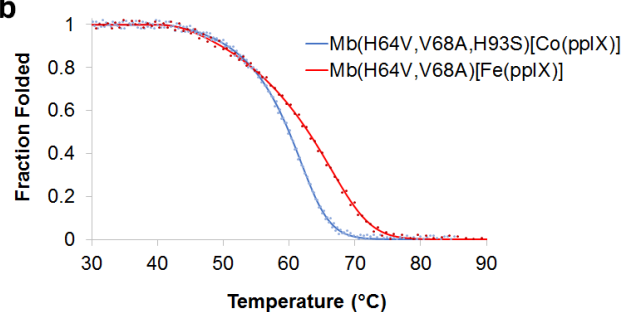


Table 5. Catalytic activity and selectivity of selected Mb(H64V,V68A) variants in the reaction with 4-(dimethylsilyl)aniline (5a) and EDA.<sup>a</sup>

En-	Protein	Cofactor	%	%	%
try			yield <sup>b</sup>	$5b^c$	$5c^c$
1	Mb(H64V,V68A)	Fe(ppIX)	72	76	1
2	Mb(H64V,V68A,H93S)	Fe(ppIX)	25	86	3
3	Mb(H64V,V68A)	Co(ppIX)	33	92	5
4	Mb(H64V,V68A,H93S)	Co(ppIX)	23	89	5

 $^{\rm a}$  Reaction conditions: 10 mM **6a**, 10 mM EDA, *E. coli* whole cells expressing Mb variants (OD<sub>600</sub> = 40) in 50 mM phosphate buffer (pH 7.2).  $^{\rm b}$  Based on GC conversion using calibration curves with isolated **5b** and **5c**.  $^{\rm c}$  The remainder to 100% corresponds to double insertion product(s).

reaction over the Si—H insertion reaction (89% selectiv.), a feature shared by the Fe-containing or histidine-ligated counterpart (86-92% selectivity; **Table 5**, Entries 2-3 vs. 4). In comparison, the parent variant Mb(H64V,V68A) is more active (72% VS. 23% vield Mb(H64V,V68A,H93S)[Co(ppIX)]) but less selective toward N—H insertion over the Si—H insertion and double insertion reactions (Table 4, Entries 1 vs. 4). From these and the previous experiments, it can be derived that the general order of reactivity for the Mb(H64V,V68A,H93S)[Co(ppIX)] variant is: C=C > N-H > Si-H. This chemoselectivity is inverted compared to that of the parent Mb variant Mb(H64V,V68A) (N—H > Si—H >> C=C) or other hemoproteins (Table 2) and organometallic catalysts (N-H >> C=C).10a-c

To evaluate the effect of the altered cofactor environment on the catalyst reactivity toward other types of Y–H insertions, further tests were carried out using 4-amino-thiophenol (6a), in which both N–H and S–H insertion reactions are possible (Table 6). Interestingly, these experiments showed that whereas Mb(H64V,V68A) favors the N–H insertion reaction (~4:1 ratio for 6b:6c; Table 6, Entries 1-2), the Mb(H64V,V68A,H93S)[Co(ppIX)] variant features inverted chemoselectivity, favoring the S–H insertion process (6b:6c ratio from 1:2 to 1:4; Table 6, Entries 3-4). In addition, Mb(H64V,V68A,H93S)[Co(ppIX)] shows higher selectivity against formation of the double insertion byproduct (0% vs. 9-15%).

Table 6. Catalytic activity and selectivity of Mb(H64V,V68A) and Mb(H64V,V68A,H93S)[Co(ppIX)] in the reaction with 4-amino-thiophenol (6a) and EDA.<sup>a</sup>

En- try	Protein	Equiv, EDA	% yield <sup>b</sup>	% 6b	% 6c	% other <sup>c</sup>
1	Mb(H64V,V68A)	1	43	73	18	9
2	Mb(H64V,V68A)	2	76	70	15	15
3	Mb(H64V,V68A,H93S) [Co(ppIX)]	1	27	20	80	0
4	Mb(H64V,V68A,H93S) [Co(ppIX)]	2	55	35	65	0

 $^a$  Reaction conditions: 3 mM  ${\bf 5a}, 3$  or 6 mM EDA, 10 mM Na<sub>2</sub>S<sub>2</sub>O<sub>4</sub>, 10 mM TCEP, 20  $\mu$ M purified Mb variant in 50 mM phosphate buffer (pH 7.2).  $^b$  Based on HPLC conversion using calibration curves with isolated  ${\bf 6b}$  and  ${\bf 6c}.$   $^c$  Double insertion product(s).

Neither Mb(H64V,V68A) nor Mb(H64V,V68A,H93S)[Co(ppIX)] were found to catalyze O-

H insertion reactions, as determined in experiments with phenol and EDA (no formation of ethyl 2-phenoxyacetate) and the lack of reactivity with water in the presence of EDA alone (no formation of ethyl 2-hydroxyacetate). This is unlike Rh- and other transition metal-based catalysts, which readily react with alcohols or water to give carbene O–H insertion products. <sup>1a,10e,19</sup>

Having identified a biocatalyst with high chemoselectivity for cyclopropanation over N-H/Si-H insertion, we were interested in examining the impact of the modified cofactor environment on the substrate scope, catalytic activity, and selectivity of this biocatalyst in olefin cyclopropanation, as compared to the parent catalyst Mb(H64V,V68A). For this purpose, we tested a panel of representative vinylarene substrates (7a-15a) previously characterized in the context of Mb(H64V,V68A)-catalyzed cyclopropanation with EDA.<sup>2a,2b</sup> As summarized in **Scheme 1**, all of these compounds could be converted by the Mb(H64V,V68A,H93S)[Co(ppIX)] variant into the corresponding cyclopropanation products **7b-15b** in moderate to good efficiency (30-88% product conversion). The results with 7b-9b indicate that substitutions at the ortho-, meta-, and para-position of the benzene ring are well tolerated by the Mb variant. Both electronrich (11a) and electrondeficient (12a) styrene derivatives were efficiently converted (70-88% yield). More sterically hindered  $\alpha$ ,  $\alpha$ -disubstituted and heterocycle-containing olefins also successfully participated in the reaction to afford the corresponding cyclopropanes 13b-15b in good yields (38-59%). Thus, despite a generally reduced catalytic activity compared to Mb(H64V,V68A),<sup>2a,2b</sup> the Mb(H64V,V68A,H93S)[Co(ppIX)] variant features a comparably broad substrate scope across structurally different vinylarenes.

the tested substrates, Mb(H64V,V68A,H93S)[Co(ppIX)] was found to favor the formation of the trans-cyclopropanation product, but with overall reduced diastereoselectivity (i.e., from 6:4 to 2:1 ratio for trans:cis) compared to Mb(H64V,V68A) (d.r. >98:2).<sup>2a,2b</sup> As an exception, **7b** was obtained with high diastereoselectivity (98:2 trans:cis). Similarly, Mb(H64V,V68A,H93S)[Co(ppIX)] maintains preference for formation of the (15,25)-configured product but with significantly reduced enantioselectivity (e.g., 11-57% ee for 7b-**11b**) compared to Mb(H64V,V68A) (95-99% ee)<sup>2a,2b</sup>, especially for the  $\alpha$ ,  $\alpha$ -disubstituted olefins (3-4% ee for 13b-15b). Interestingly, parallel experiments Mb(H64V,V68A)[Co(ppIX)] showed that this metallo-substituted variant displays higher trans-(15,25)-selectivity in reactions compared Mb(H64V,V68A,H93S)[Co(ppIX)] (Scheme S1). Thus, the general reduction in stereoselectivity observed with Mb(H64V,V68A,H93S)[Co(ppIX)] vs. Mb(H64V,V68A) can be attributed to both the metal substitution and the mutation of the proximal ligand (His→Ser). This result is not entirely surprising, given that (a) the active site mutations in Mb(H64V,V68A) were optimized for high trans-(1S,2S)-selectivity in the presence of the native histidine-ligated heme cofactor, and (b) both the metal substitution and the structural change induced by the His93→Ser substitution are likely to alter the orientation of the metalloporphyrin within the core of the protein, thereby affecting the asymmetric induction effect imposed by the protein scaffold during this reaction. Indeed, a significant shift in diastereose-lectivity for styrene cyclopropanation with EDA was also noted upon substitution of the proximal cysteine with serine in a cytochrome P450 enzyme (22:78 vs. 76:24 cis:trans, respectively).<sup>3b</sup> Altogether, the results above showed that Mb(H64V,V68A,H93S)[Co(ppIX)] could be successfully applied to the cyclopropanation of a variety of aryl-substituted olefins, albeit re-optimization of its active site would be required for enhancing its stereoselectivity,

# Scheme 1. Substrate scope for Mb(H64V,V68A,H93S)[(Co(ppIX)]-catalyzed cyclopropanation of vinylarenes with EDA.<sup>a</sup>

Mb(H64V,V68A,H93S)[Co(ppIX)]

<sup>a</sup> Reaction conditions: 10 mM olefin, 20 mM EDA, *E. coli* whole cells expressing Mb variants ( $OD_{600}$  = 80) in 50 mM phosphate buffer (pH 7.2). <sup>b</sup> Based on GC conversion. <sup>c</sup> For *trans-*(1*S*,2*S*) product. <sup>d</sup> Using 5 mM olefin and 10 mM EDA. Enantiomeric excess not determined.

14b

(38%; 174 TON;

d.r. 66:34; 4% ee)

15b

(56%; 255 TON;

d.r. 67:33; 3% ee)

### Conclusion

13b

(59%; 269 TON;

d.r. 67:33; 4% ee)

In summary, we have developed a novel biocatalytic strategy, based on an engineered myoglobin-based carbene transferase, for the chemoselective cyclopropanation of ole-fin substrates bearing unprotected Y—H groups (Y= N, Si). This transformation, unattainable using previously available carbene transfer (bio)catalysts, opens the way to the selective carbene-mediated functionalization of olefins in the presence of inherently more reactive Y—H groups. As emerged from the analysis of a systematic library of cofactor modified Mb variants, the unique and atypical reactivity of Mb(H64V,V68A,H93S)[Co(ppIX)] compared to Mb and other hemoproteins is specifically induced by the combination of a non-native metal (Co) and non-native residue (Ser)

at the proximal axial site of the metalloporphyrin cofactor. While featuring inverted chemoselectivity in carbene transfer reactions compared to the histidine-ligated Fe-containing counterpart (i.e., C=C > N-H > Si-H vs. N-H > Si-H >> C=CN-H and S-H vs. N-H Mb(H64V,V68A,H93S)[Co(ppIX)] features comparable stability, ease of expression in E. coli, and broad substrate scope in the cyclopropanation of vinylarenes with EDA. Further engineering of this scaffold (e.g., through active site mutagenesis)<sup>2a,2b</sup> is expected to improve its stereoselectivity, which is currently modest. The present studies highlight the functional plasticity of myoglobin as a carbene transferase and illustrate how modulation of the cofactor environment within this metalloprotein scaffold can provide a promising strategy for tuning its reactivity in the context of abiotic carbene transfer reactions. Further studies are warranted to elucidate the factors underlying the atypical reactivity of the Mb(H64V,V68A,H93S)[Co(ppIX)] catalyst.

### **Experimental Section**

General Information. All chemicals and reagents were purchased from commercial suppliers (Sigma-Aldrich, Alfa Aesar, TCI, Oakwood Chemicals, Combi Blocks) and used without any further purification, unless otherwise stated. EDA was purchased from Sigma-Aldrich as 87% m/v solution in dichloromethane. Dimethyl(4-vinylphenyl)silane 3a and 4-(dimethylsilyl)aniline 4a were synthesized according to a previously reported procedure.<sup>6</sup> Authentic racemic standards for the cyclopropanation products 7b-15b and **20b** were synthesized and characterized as described previously.<sup>2a,2b</sup> All dry organic reactions were carried out under argon in oven-dried glassware with magnetic stirring using standard gas-tight syringes, cannulae and septa. <sup>1</sup>H and <sup>13</sup>C NMR spectra were measured on Bruker DPX-400 (operating at 400 MHz for <sup>1</sup>H and 100 MHz for <sup>13</sup>C) or Bruker DPX-500 (operating at 500 MHz for <sup>1</sup>H and 125 MHz for <sup>13</sup>C). Tetramethylsilane (TMS) served as the internal standard (0 ppm) for <sup>1</sup>H NMR and the residual proton signal of the solvents was used as the internal standard for <sup>13</sup>C NMR. HRMS analyses were performed using a Q Exactive Plus Mass Spectrometer at the Proteomics Facility of the University of Rochester. Silica gel chromatography purifications were carried out using AMD Silica Gel 60 230-400 mesh. Thin Layer Chromatography (TLC) were carried out using Merck Millipore TLC silica gel 60 F254 glass plates.

**Growth Media.** Enriched M9 media was prepared as follows. For 1 L, 770 mL deionized H<sub>2</sub>O was added with 200 mL M9 salts (5x) solution, 20 mL glucose (20% m/v), 10 mL casamino acids (20% m/v), 1 mL MgSO<sub>4</sub> (2 M), and 100  $\mu$ L CaCl<sub>2</sub> (1 M). The M9 salts (5x) solution was prepared by dissolving 34 g Na<sub>2</sub>HPO<sub>4</sub>, 15 g K<sub>2</sub>HPO<sub>4</sub>, 2.5 g NaCl, 5 g NH<sub>4</sub>Cl in 1 L deionized H<sub>2</sub>O and sterilized by autoclaving. The casamino acids and MgSO<sub>4</sub> solutions were autoclaved separately. The CaCl<sub>2</sub> and glucose stock solutions were sterilized by filtration. Enriched M9 agar plates were prepared by adding 17 g agar to 1 L of enriched M9 media containing all of the aforementioned components at the specified concentrations with the exception of glucose and CaCl<sub>2</sub>, which were added immediately prior to plating. To media and plates, ampicillin was added to a final concentration of 100 mg/L

and chloramphenicol was added to a final concentration of 34 mg/L.

Recombinant expression of myoglobins containing artificial metalloporphyrins. All myoglobin variants were expressed from pET22-based vectors containing the target gene under a T7 promoter. The recombinant protein was engineered with a C-terminal polyhistidine tag. E. coli C41(DE3) cells expressing the heme transporter ChuA (T7 promoter) and GroES/EL chaperon proteins (araBAD promoter) were prepared via transformation with the plasmid pGroES/EL-ChuA.<sup>16</sup> E. coli C41(DE3) cells containing the pGroES/EL-ChuA plasmid were transformed with the pET22 vector encoding the desired Mb variant and selected on M9 agar plates containing ampicillin (100 mg/L) and chloramphenicol (34 mg/L). Single colonies were used to inoculate 5 mL of enriched M9 media supplemented with ampicillin and chloramphenicol followed by incubation at 37°C with shaking (180 rpm) for 10 to 15 hours. At an OD<sub>600</sub> of 0.8 to 1.0, the desired cofactor was added directly to the expression culture to a final concentration of about 30 mg/L followed by induction of protein expression with IPTG and arabinose at final concentrations of 1 mM. Cells were incubated at 20°C with shaking (180 rpm) for 20 to 24 hours. After harvesting, the cell pellets were resuspended in 20 mL of Ni NTA Lysis Buffer (50 mM KPi, 250 mM NaCl, 10 mM histidine, pH = 8.0) lysed by sonication, and clarified by centrifugation (14,000 rpm, 4°C, 30 min). When using E. coli in whole cell reactions, harvested cells were resuspended in 50 mM KPi pH 7.2 and stored at 4°C for no longer than 12 hours.

**Protein Purification.** Clarified lysate was transferred to a Ni-NTA column equilibrated with Ni-NTA Lysis Buffer. The resin was washed with 50 mL of Ni-NTA Lysis Buffer followed by 50 mL of Ni-NTA Wash Buffer (50 mM KPi, 250 mM NaCl, 20 mM Histidine, pH = 8.0). Proteins were eluted with Ni-NTA Elution Buffer (50 mM KPi, 250 mM NaCl, 250 mM Histidine, pH = 7.0). After elution from the Ni-NTA column, the protein was buffer exchanged against 50 mM KPi buffer (pH 7.0) using 10 kDa Centricon filters. The concentrations of the Mb variants were calculated using the following extinction coefficients:  $\epsilon_{410} = 157 \text{ mM}^{-1} \text{ cm}^{-1}$  for Fe(ppIX)-containing variants,  $\epsilon_{470} = 60 \text{ mM}^{-1} \text{ cm}^{-1}$  for Co(ppIX)-containing variants, and  $\epsilon_{405} = 122 \text{ mM}^{-1} \text{ cm}^{-1}$  for Rh(mpIX)-containing variants.

General Procedure for Biocatalytic Reactions with Whole Cells and Purified Protein. Under standard reaction conditions, 500 µL-scale reactions were carried out using 10-20 µM Mb variant, 10 mM substrate, 10 mM EDA and 10 mM sodium dithionite. TCEP (10 mM) was also added to the reactions with 6a to prevent disulfide formation. In a typical procedure, a solution containing the desired myoglobin variant in potassium phosphate buffer (50 mM, pH 7.0) with sodium dithionite was prepared in an anaerobic chamber. Reactions were initiated by addition of 10 µL of olefin followed by the addition of 10 µL of EDA from 0.5 M stock solutions, and the reaction mixtures were stirred in the chamber for 12 hours at room temperature. Whole-cell reactions were performed using *E. coli* C41(DE3) cells prepared using the method described above. Cell suspensions were transferred to an anaerobic chamber and diluted to

the indicated cell density (OD $_{600}$ : 40-80) with 50 mM KPi pH 7.2. Reactions were initiated by addition of 10  $\mu$ L of olefin followed by the addition of 10  $\mu$ L of EDA from 0.5 M stock solutions, and the mixtures were stirred in the chamber for 12 hours at room temperature.

Product Analysis. The reactions with 1a, 3a, 4a, and 5a were analyzed by adding 20 µL of internal standard (benzodioxole, 50 mM in ethanol) to the reaction mixture, followed by extraction with 400 µL of dichloromethane and analysis by gas chromatography (GC). GC analyses were carried out using a Shimadzu GC-2010 gas chromatograph equipped with a FID detector and a Chiral Cyclosil-B column (30 m x 0.25 mm x 0.25 µm film). Separation method: 1 µL injection, injector temp.: 200 °C, detector temp: 300 °C. Gradient: column temperature set at 120 °C for 3 min, then to 150 °C at 0.8 °C/min, then to 245°C at 25 °C/min. Total run time was 28.60 min. For the reactions with 6a, the DCM extraction solution was evaporated and the residue was redissolved in 300 uL methanol containing 10 mM TCEP, followed by HPLC analysis using a Shimadzu LC-2010A instrument equipped with a UV-vis detector. Analytical conditions: Thermo Fisher Scientific Hypersil GOLD C<sub>18</sub> column (250 x 4.6 mm); UV detection: 254 nm; flow rate: 1.0 mL/min: solvent A: 1% trifluoroacetic acid in H<sub>2</sub>O; solvent B: 1% trifluoroacetic acid in acetonitrile; gradient: 0-3 min: 30% B; 3-21 mins: 30% B to 90% B; 21-24 mins: 90% B; 24-24.5 mins: 90% B to 30% B; 24.5-30 mins: 30% B. Retention times: 3.82 min for 4-aminothiophenol; 4.89 min for S-H insertion product; 13.57 min for N-H insertion product; 14.91 min for double insertion product. Calibration curves for quantification of each single insertion product were constructed using authentic standards prepared synthetically or enzymatically as described above. All measurements were performed at least in duplicate.

CD analyses and T<sub>m</sub> Determination. Circular dichroism (CD) spectroscopy and thermal denaturation analysis were performed using a JASCO J-1100 CD spectrophotometer equipped with variable temperature/wavelength denaturation software. Far UV CD spectra (250-190 nm) were obtained using 3 µM solutions of purified Mb variant in 50 mM potassium phosphate buffer (pH 7.0) and recorded at 20°C at a scan rate of 50 nm/min with a bandwidth of 1 nm and an averaging time of 10 seconds per measurement. Thermal denaturation curves were measured by monitoring the change in molar ellipticity at 222 nm ( $\theta_{222}$ ) over a temperature range from 20°C to 100°C. The temperature increase was set to 0.5°C per minute with an equilibration time of 10 seconds. Data integration time for the melt curve was set to 4 seconds with a bandwidth of 1 nm. Linear baselines for the folded  $(\theta_f)$  and unfolded state  $(\theta_u)$  were generated. Melting temperature (T<sub>m</sub>) was determined using the low temperature ( $\theta_f = m_f T + b_f$ ) and high temperature ( $\theta_u = m_u T +$ bu) equations fitted to the experimental data before and after global unfolding, respectively. These data were normalized and converted to fraction of folded protein (F<sub>f</sub>) vs. temperature plots and the resulting curve was fitted to a sigmoidal equation ( $\theta_{fit}$ ) via nonlinear regression analysis in SigmaPlot, from which apparent melting temperatures were derived.

Ethyl 2-(dimethyl(phenyl)silyl)acetate (1b). Ethyl 2-(dimethyl(phenyl)silyl)acetate 1b was synthesized according to a modification of a reported procedure.6 Dimethyl(phenyl)silane 1a (136 mg, 2.00 mmol, 1 equiv.) and Rh<sub>2</sub>(OAc)<sub>4</sub> (4.4 mg, 10 μmol, 1 mol%) were added to a flame dried 10 mL round bottom flask under argon atmosphere. dissolved in anhydrous DCM (4 mL), and subsequently cooled to -78 °C. A solution of EDA (87%, 131 mg, 1.00 mmol, 1 equiv.) in anhydrous DCM (1 mL) was added dropwise with a syringe pump over a period of 30 min. The reaction mixture was allowed to reach room temperature and stirred for 16 h. The solvent was removed under reduced pressure and the crude product purified via column chromatography on silica gel (0-7.5% EtOAc/pentanes) to yield ethyl 2-(dimethyl(phenyl)silyl)acetate 1b as a clear oil (99.4 mg, 0.45 mmol, 45% yield).  $R_f = 0.34$  (7.5% EtOAc/pentanes). <sup>1</sup>H NMR (CDCl<sub>3</sub>, 500 MHz): δ 7.51 (m, 2H), 7.34 (m, 3H), 3.98 (q, J = 7.2, 2H), 2.06 (s, 2H), 1.12 (t, J = 7.0Hz, 3H), 0.36 (s, 6H). <sup>13</sup>C NMR (CDCl<sub>3</sub>, 125 MHz): δ 172.7, 137.7, 134.1, 130.0, 128.4, 60.4, 26.7, 14.7, -2.6. GC-MS m/z (% relative intensity): 207 (46.5), 177 (29.9), 165 (84.3), 145 (71.6), 135 (100.0)

Ethyl 2-(4-(dimethylsilyl)phenyl)cyclopropanecarboxylate (3b). E. coli C41(DE3) cells expressing the variant Mb(H64V,V68A,H93S)[Co(ppIX)] were prepared and harvested according to the protocol described above. In an anaerobic chamber (0 ppm O2, 2.5% H2 atmosphere), the whole cell suspension was diluted to an  $OD_{600}$  of 80 with argon purged in phosphate buffer (50 mM, pH 7.2). A solution of dimethyl (4-vinylphenyl) silane 3a (50.0 mg, 0.31 mmol, 1 equiv.) in methanol (0.75 mL) was added dropwise and while stirring to 28.5 mL of the whole cell suspension in an Erlenmeyer flask. The reaction was initiated by the dropwise addition of a solution of EDA (87%, 29.5 mg, 0.23 mmol, 0.75 equiv.) in methanol (0.75 mL). The reaction mixture was stirred at room temperature for 16 hours and extracted with DCM (3x30 mL). The combined organic layers were dried over sodium sulfate and concentrated under reduced pressure. The crude product was purified by column chromatography on silica gel (0-7.5% Et<sub>2</sub>0/pentanes) and the fractions analyzed by gas chromatography with chiral column to separate the cis- (4.5 mg, 0.017 mmol, 1%) **3b**-cis and trans-isomers (3.9 mg, 0.015 mmol, 1%) 3b-trans and as clear oils. The configuration of **3b** was assigned by comparison to the splitting pattern in the <sup>1</sup>H NMR in alignment with the previously determined cis and trans isomers of **10b** (see supporting information). **3b**-cis:  $R_f = 0.44$  (7.5%) Et<sub>2</sub>O/pentanes). <sup>1</sup>H NMR (CD<sub>2</sub>Cl<sub>2</sub>, 500 MHz):  $\delta$  7.43 (d, J = 8.0 Hz, 2H), 7.08 (d, I = 7.5 Hz, 2H), 4.36 (m, 1H), 4.11 (q, I = 7.2Hz, 2H), 4.45 (m, 1H), 1.87 (m. 1H), 1.54 (m, 1H), 1.29 (m, 1H), 1.23 (t, J = 7.0 Hz, 3H), 0.30 (d, J = 4.0 Hz, 6H). <sup>13</sup>C NMR (CD<sub>2</sub>Cl<sub>2</sub>, 125 MHz): δ 171.2, 138.6, 135.8, 134.1, 129.4, 60.6, 25.9, 22.2, 14.4, 11.5, -3.6. GC-MS *m/z* (% relative intensity): 248 (79.0), 233 (33.0), 201 (44.6), 144 (55.6), 129 (59.8), 115 (100.0). **3b**-trans:  $R_f = 0.61$  (7.5%  $Et_2O$ /pentanes). <sup>1</sup>H NMR (CD<sub>2</sub>Cl<sub>2</sub>, 500 MHz):  $\delta$  7.43 (d, I = 8.0 Hz, 2H), 7.08 (d, I = 7.5 Hz, 2H, 4.36 (m, 1H), 4.11 (q, J = 7.2 Hz, 2H), 4.45 (m, 1H)1H), 1.87 (m. 1H), 1.54 (m, 1H), 1.29 (m, 1H), 1.23 (t, J = 7.0 Hz, 3H), 0.30 (d, J = 4.0 Hz, 6H).  $^{13}$ C NMR (CD<sub>2</sub>Cl<sub>2</sub>, 125 MHz): δ 173.5, 142.0, 135.8, 134.7, 126.2, 61.2, 26.5, 24.8, 17.4, 14.6, -3.5. GC-MS m/z (% relative intensity): 248 (83.3), 233

(33.5), 201 (43.7), 114 (56.6), 129 (62.7), 115 (100.0). HRMS (ESI) m/z: [M + H]<sup>+</sup> Calcd. For  $C_{14}H_{21}O_2Si$  249.1311; Found 249.1303.

Ethyl 2-(dimethyl(4-vinylphenyl)silyl)acetate (3c). Ethyl 2-(dimethyl(4-vinylphenyl)silyl)acetate 3c was synthesized according to a modification of a previously reported procedure.6 Dimethyl(4-vinylphenyl)silane 3a (150 mg, 0.92 mmol, 1 equiv.) and Rh<sub>2</sub>(OAc)<sub>4</sub> (4.0 mg, 9 µmol, 1 mol%) were added to a flame dried 10 mL round bottom flask under argon atmosphere, dissolved in anhydrous DCM (4 mL), and subsequently cooled to -78 °C. A solution of EDA (106 mg, 0.9 mmol, 1 equiv.) in anhydrous DCM (1 mL) was added dropwise with a syringe pump over a period of 30 min. The reaction mixture was allowed to reach room temperature and stirred for 16 h. The solvent was removed under reduced pressure and the crude product purified via column chromatography on silica gel (0-4% yield ethyl 2-(dimethyl(4-vi-EtOAc/hexanes) to nylphenyl)silyl)acetate 3c as a clear oil (36.7 mg, 0.15 mmol, 15% yield).  $R_f = 0.48$  (4% EtOAc/hexanes). <sup>1</sup>H NMR (CDCl<sub>3</sub>, 500 MHz):  $\delta$  7.50 (d, I = 8.0, 2H), 7.41 (d, I = 8.0, 2H), 6.72 (dd, I = 11.0, 17.5, 1H), 5.79 (d, I = 17.5, 1H), 5.28 (d, J = 11.0, 1H), 4.05 (q, J = 7.2, 2H), 2.11 (s, 2H), 2.27 (t, J = 11.0, 2H), 2.27 (t, J = 11.0, 2H), 2.27 (t, J = 2.11), 2.27 (t, J = 2.11),7.3 Hz, 3H), 0.40 (s, 6H).  $^{13}$ C NMR (CDCl<sub>3</sub>, 125 MHz):  $\delta$  172.7, 138.8, 136.8, 133.9, 129.0, 125.8, 114.7, 60.1, 26.4, 14.5, 2.6. GC-MS m/z (% relative intensity): 233 (76.6), 191 (87.2), 163 (44.2), 161 (100.0), 147 (39.7), 145 (42.7). HRMS (ESI) m/z: [M + H]+ Caldc for  $C_{14}H_{21}O_2Si$  249.1311; Found 249.1306.

Ethyl 2-(4-aminophenyl)cyclopropanecarboxylate (4b). Compound 4b was prepared according to the procedure described in Scheme S2. Di-tert-butyl dicarbonate/Boc<sub>2</sub>O (1.174 g, 5.38 mmol. 3.2 equiv.) and N<sub>1</sub>Ndiisopropylethyl-amine/DIPEA (651 mg. 5.04 mmol, 3 equiv.) were added to a solution of dimethyl(4-vinylphenyl)silane 3a (200 mg, 1.68 mmol, 1 equiv.) in DCM (30 mL). The reaction mixture was stirred over night at room temperature and, after that, refluxed at 40 °C until completion, which was monitored by TLC. To remove excess Boc20, the solvent was evaporated and the crude residue taken up in 10 mL of a 1:1 mixture of THF:water before addition of glycine (246 mg, 4.30 mmol) and Na<sub>2</sub>CO<sub>3</sub> (910 mg, 8.60 mmol). After stirring overnight, THF was removed in vacuo and the aqueous layer extracted with DCM (3x10 mL). The combined organic layers were washed with brine (10 mL), dried over sodium sulfate, filtered and concentrated under reduced pressure. Flash column chromatography on silica gel (25% Et<sub>2</sub>O/pentanes) furnished tertbutyl (4-vinylphenyl)carbamate 16 as white flaky solid (284 mg, 1.29 mmol, 77 % yield).  $R_f = 0.63$  (25%  $Et_2O/pen$ tanes). <sup>1</sup>H NMR (CDCl<sub>3</sub>, 500 MHz): δ 7.30-7.19 (m, 4H), 6.59 (dd, J = 11.0, 17.5 Hz, 1H) 6.43 (br, 1H), 5.58 (d, J = 17.5 Hz, 1H), 5.09 (d, J = 11.0 Hz, 1H), 1.45 (s, 9H). GC-MS m/z (% relative intensity): 219 (19.4), 163 (100.0), 119 (76.9).

To a flame dried 10 mL round bottom flask, equipped with a stir bar, were added tert-butyl (4-vinylphenyl)carbamate **16** (100 mg, 0.46 mmol, 1 equiv.),  $Rh_2(OAc)_4$  (4.0 mg, 9  $\mu$ mol, 2 mol%) and anhydrous DCM (2.5 mL) under argon. After that, a solution of EDA (87%, 119 mg, 0.9 mmol, 2

equiv.) in anhydrous DCM (2.5 mL) was slowly added dropwise with a syringe pump over a period of 4 hours. The resulting reaction mixture was stirred at room temperature for 12 hours, after which the solvent was removed under reduced pressure and the crude product purified via column chromatography on silica gel (0-20% Et<sub>2</sub>0/pentanes) to afford ethyl 2-(4-((tert-butoxycarbonyl)amino)phenyl)cyclopropanecarboxylate 17 as a colorless oil (23 mg, 0.075 mmol, 16% yield).  $R_f = 0.36 (25\% \text{ Et}_2\text{O/pentanes})$ . <sup>1</sup>H NMR (CDCl<sub>3</sub>, 500 MHz):  $\delta$  7.26 (d, J = 10.5 Hz, 2H), 7.02 (d, J = 10.5 Hz, 2H, 6.48 (br, 1H), 4.16 (q, J = 9.0 Hz, 2H), 2.47 (m, m)1H), 1.83 (m, 1H), 1.54 (m, 1H), 1.51 (s, 9H), 1.28 (t, J = 9.0 Hz, 3H), 1.26 (m, 1H). <sup>13</sup>C NMR (CDCl<sub>3</sub>, 125 MHz): δ 173.6, 152.9, 137.0, 134.8, 126.9, 118.8, 80.6, 60.8, 28.5, 25.9, 24.1, 17.0, 14.4. GC-MS m/z (% relative intensity): 305 (16.8), 249 (70.2), 205 (22.1), 176 (51.2), 158 (36.6), 132 (100.0).

A solution of 2-(4-((tert-butoxycarbonyl)amino)phenyl)cyclopropanecarboxylate 17 (20 mg, 0.065 mmol, 1 equiv.) in DCM (0.5 mL) was cooled to 0 °C. Trifluoroacetic acid (0.5 mL) was added dropwise and the reaction mixture stirred for 2 hours before removing the solvent under reduced pressure. The crude product was taken up in 1.5 mL DCM, transferred to an Eppendorf tube and washed with NaHCO<sub>3</sub> (1 mL). The aqueous layer was extracted with DCM (2x1 mL) and the combined organic layers were dried over sodium sulfate, centrifuged, the supernatant decanted and the solvent removed in vacuo to yield ethyl 2-(4-aminophenyl)cyclopropanecarboxylate 4b as yellow solid (11.3 mg, 0.055 mmol, 85 % yield). R<sub>f</sub> = 0.43 (40% EtOAc/hexanes). <sup>1</sup>H NMR (CDCl<sub>3</sub>, 500 MHz):  $\delta$  6.91 (d, J = 8.0 Hz, 2H), 6.61 (d, J = 8.5 Hz, 2H), 4.16 (q, J = 7.0, 2H), 3.60 (br, 2H), 2.43 (m, 1H), 1.79 (m, 1H), 1.52 (m, 1H), 1.27 (t, J = 7.0 Hz, 3H), 1.23 (m, 1H). <sup>13</sup>C NMR (CDCl<sub>3</sub>, 125 MHz): δ 173.9, 145.1, 130.0, 127.4. 115.3. 60.7. 26.0. 23.9. 16.7. 14.4. GC-MS m/z (% relative intensity): 205 (44.0), 176 (23.6), 160 (21.1), 132 (100.0).

Ethyl 2-((4-vinylphenyl)amino)acetate (4c). E. coli C41(DE3) cells expressing the Mb(H64V,V68A,H93C) were prepared and harvested according to the protocol described above. In an anaerobic chamber (0 ppm O<sub>2</sub>, 2.5% H<sub>2</sub> atmosphere), the whole cell suspension was diluted to an OD<sub>600</sub> of 80 with argon-purged 50 mM phosphate buffer (pH 7.2). A solution of 4-vinylaniline 4a (48.0 mg, 0.40 mmol, 1 equiv.) in methanol (1.0 mL) was added dropwise and while stirring to 38 mL of the whole cell suspension in an Erlenmeyer flask. The reaction was initiated by the dropwise addition of a solution of EDA (87%, 52.4 mg, 0.40 mmol, 1 equiv.) in methanol (1.0 mL). The reaction mixture was stirred at room temperature for 16 hours and extracted with DCM (3x40 mL). The combined organic layers were dried over sodium sulfate and concentrated under reduced pressure. The crude product was purified by column chromatography on silica gel (0-20% Et<sub>2</sub>O/pentanes) to yield ethyl 2-((4-vinylphenyl)amino)acetate **4c** (20.0 mg, 0.10 mmol, 25%) as white solid.  $R_f = 0.31$ (20% Et<sub>2</sub>O/pentanes). <sup>1</sup>H NMR (CDCl<sub>3</sub>, 500 MHz):  $\delta$  7.23 (d. J = 8.0 Hz, 2H), 6.53 (d, J = 8.0 Hz, 2H), 5.51 (d, J = 17.5 Hz, 1H), 5.01 (d, J = 10.5 Hz, 1H), 4.32 (br, 1H), 4.21 (q, J = 6.7 Hz, 2H), 3.87 (d, J = 4.5 Hz, 2H), 1.27 (t, J = 7.0 Hz, 3H). <sup>13</sup>C NMR (CDCl<sub>3</sub>, 125 MHz): δ 171.1, 146.9, 136.7, 128.1, 127.5, 113.0,

111.0, 61.5, 45.9, 14.3. GC-MS m/z (% relative intensity): 205 (25.8), 132 (100.0).

Ethyl 2-((4-(dimethylsilyl)phenyl)amino)acetate (5b). E. coli C41(DE3) cells expressing the variant Mb(H64V,V68A) were prepared and harvested according to the protocol described above. Under argon atmosphere, the cells were resuspended in argon purged 50 mM phosphate buffer (pH 7.2) and diluted to an OD<sub>600</sub> of 40. A solution of 4-(dimethylsilyl)aniline **5a** (60.5 mg, 0.40 mmol, 1 equiv.) in ethanol (1.0 mL) was added dropwise and while stirring to 38 mL of the whole cell suspension in an Erlenmeyer flask. A solution of EDA (87%, 52.6 mg, 0.40 mmol, 1 equiv.) in ethanol (1.0 mL) was added dropwise over 4 hours. The reaction mixture was stirred at room temperature for 16 hours and extracted with DCM (3x40 mL). The combined organic layers were dried over sodium sulfate and concentrated under reduced pressure. The crude product was purified by column chromatography on silica gel (0-20% EtOAc/hexanes) to yield ethyl 2-(4-(dimethylsilyl)-phenyl)cyclopropanecarboxylate **5b** (40.0 mg, 0.17 mmol, 42%) as clear oil.  $R_f = 0.48$  (20% EtOAc/hexanes). <sup>1</sup>H NMR (CDCl<sub>3</sub>, 500 MHz):  $\delta$  7.37 (d, J = 8.5 Hz, 2H), 6.62 (d, J = 8.5 Hz, 2H), 4.39 (m, 1H), 4.26 (q, J = 7.0 Hz, 2H), 3.91 (s, 2H), 1.31 (t, J = 7.3 Hz, 3H), 0.30 (d, J = 3.5 Hz, 6H). <sup>13</sup>C NMR (CDCl<sub>3</sub>, 125 MHz): δ 171.1, 148.0, 135.4, 124.8, 122.8, 61.5, 45.7, 14.3, -3.3. GC-MS m/z (% relative intensity): 237 (32.5), 164 (100.0). HRMS (ESI) m/z: [M + H]<sup>+</sup> Calcd for C<sub>12</sub>H<sub>20</sub>NO<sub>2</sub>Si 238.1263; Found 238.1260.

Ethyl 2-((4-aminophenyl)dimethylsilyl)acetate (5c). Compound 5c was prepared according to the procedure described in **Scheme S3**, which was adapted from a previously reported procedure.<sup>6</sup> A solution of 4-(dimethylsilyl)aniline **5a** (50 mg, 0.33 mmol, 1 equiv.) and pyridine (52 mg, 0.66 mmol, 2 equiv.) in anhydrous DCM (1 mL) was stirred for 10 min, followed by the addition of benzyl chloroformate (68 mg, 0.40 mmol, 1.2 equiv.). The reaction mixture was stirred overnight, after which the solvent was removed under reduced pressure. Benzyl (4-(dimethylsilyl)phenyl)carbamate 18 was obtained as a white flaky solid (62 mg, 0.22 mmol, 66% yield) after purification by column chromatography on silica gel (5% EtOAc/hexanes).  $R_f = 0.38$  (5% EtOAc/hexanes). <sup>1</sup>H NMR (CDCl<sub>3</sub>, 500 MHz):  $\delta$ 7.49-7.35 (m, 9H), 6.71 (br, 1H), 5.21 (s, 2H), 4.41 (quin, J =3.5 Hz, 1H), 0.33 (d, J = 3.5 Hz, 6H). <sup>13</sup>C NMR (CDCl<sub>3</sub>, 125 MHz): δ 153.3, 138.9, 136.1, 135.1, 132.0, 128.8, 128.5, 128.5, 118.2, 67.2, -3.5. GC-MS m/z (% relative intensity): 285 (82.5), 241 (25.9), 226 (34.0), 162 (51.7), 150 (100.0).

Benzyl (4-(dimethylsilyl)phenyl)carbamate 18 (50 mg, 0.18 mmol, 1 equiv.) and  $Rh_2(OAc)_4$  (1 mg, 2  $\mu$ mol, 1 mol%) were added to a flame dried 5 mL round bottom flask under argon atmosphere, dissolved in anhydrous DCM (1 mL), and subsequently cooled to -78 °C. A solution of EDA (23.6 mg, 0.18 mmol, 1 equiv.) in anhydrous DCM (1 mL) was added dropwise with a syringe pump over a period of 30 min. The reaction mixture was allowed to reach room temperature and stirred for 16 h. The solvent was removed under reduced pressure and the crude product purified via column chromatography on silica gel (0-20% EtOAc/hexanes) to afford ethyl 2-((4-(((benzyloxy)carbonyl)amino)phenyl)dimethylsilyl)acetate 19 as a clear oil (6.0 mg, 0.018 mmol,

9% yield).  $R_f$  = 0.49 (20% EtOAc/hexanes). <sup>1</sup>H NMR (CDCl<sub>3</sub>, 400 MHz):  $\delta$  7.48-7.34 (m, 9H), 6.70 (br, 1H), 5.20 (s, 2H), 4.03 (q, J = 7.1 Hz, 2H). 2.08 (s, 2H), 1.16 (t, J = 7.1 Hz, 3H), 0.38 (s, 6H). <sup>13</sup>C NMR (CDCl<sub>3</sub>, 125 MHz):  $\delta$  172.8, 153.2, 130.1, 136.1, 134.7, 131.5, 128.8, 128.6, 128.5, 118.1, 67.3, 60.1, 26.5, 14.5, -2.6. APCI-MS (TLC) m/z: 372, 284.

A flame dried 5 mL round bottom flask was charged with 2-((4-(((benzyloxy)carbonyl)amino)phenyl)dimethylsilyl)acetate **19** (10 mg, 0.027 mmol, 1 equiv.), 10% Pd/C (4 mg) and anhydrous EtOH (1 mL) under argon atmosphere. The reaction mixture was purged with H<sub>2</sub> for 30 min and stirred overnight under H<sub>2</sub> atmosphere. After exchanging the atmosphere with argon, the residue was diluted with EtOAc, filtered over celite, concentrated under reduced pressure and purified by column chromatography on silica gel (10-50% EtOAc/hexanes) to give ethyl 2-((4aminophenyl)dimethylsilyl)acetate 5c as yellow oil (4.1 mg, 0.017 mmol, 64 %).  $R_f = 0.55$  (50% EtOAc/hexanes). <sup>1</sup>H NMR (CDCl<sub>3</sub>, 500 MHz):  $\delta$  6.96 (d, J = 5.0, 2H), 6.59 (d, J = 5.0 Hz, 2H), 4.24 (q, J = 5.0 Hz, 2H), 2.67 (s, 2H), 1.95 (t, J = 5.0Hz, 3H), 1.31 (s, 6H). <sup>13</sup>C NMR spectrum could not be collected due to the instability of the product 5c in the NMR solvent. GC-MS m/z (% relative intensity): 237 (20.6), 222 (27.4), 180 (69.1), 150 (100.0), 136 (31.8). HRMS (ESI) *m/z*: [M + H]<sup>+</sup> Calcd for C<sub>12</sub>H<sub>20</sub>NO<sub>2</sub>Si 238.1263; Found 238.1256.

Ethyl 2-((4-mercaptophenyl)amino)acetate (6b). This compound was synthesized according to a modification of a previously reported procedure (Scheme S4).  $^{20}$  4-Aminothiophenol 6a (200 mg, 1.60 mmol, 1 equiv.) was dissolved in a minimal amount of MeOH (2 mL) and DMSO (60  $\mu$ L) and treated with I<sub>2</sub> (162 mg, 0.64 mmol, 0.4 equiv.). After consumption of the starting material (3 h), the solvent was removed under reduced pressure and the crude product purified by column chromatography on silica gel (20-80% EtOAc/hexanes) to yield 4,4'-disulfanediyldianiline (20) as yellow solid (104 mg, 0.42 mmol, 52% yield).  $R_f$  = 0.26 (50% EtOAc/hexanes).  $^1$ H NMR (CDCl<sub>3</sub>, 500 MHz):  $\delta$  7.22 (d, J = 7.0 Hz, 2H), 6.55 (d, J = 8.5 Hz, 2H), 3.75 (br, 4H).  $^{13}$ C NMR (CDCl<sub>3</sub>, 125 MHz):  $\delta$  147.7, 134.4, 124.7, 115.5. GC-MS m/z (% relative intensity): 248 (38.5), 124 (78.9), 125 (100.0).

Ethyl 2-((4-mercaptophenyl)amino)acetate. To a flame dried 10 mL round bottom flask, equipped with a stir bar, were added 4,4'-disulfanediyldianiline 20 (48 mg, 0.19 mmol, 1 equiv.), Rh<sub>2</sub>(OAc)<sub>4</sub> (2 mg, 4 µmol, 2 mol%), and anhydrous DCM (1 mL) under argon. After that, a solution of EDA (43 mg, 0.38 mmol, 2 equiv.) in anhydrous DCM (1 mL) was slowly added dropwise over a period of 30 min. The resulting reaction mixture was stirred at room temperature for 16 hours. The solvent was removed under reduced pressure and the crude product purified via column chromatography on silica gel (20-80% EtOAc/hexanes) to afford ethyl 2-((4-mercaptophenyl)amino)acetate (6b) as a yellow solid (20 mg, 0.089 mmol, 47% yield). R<sub>f</sub> = 0.31 (50% EtOAc/hexanes). 1H NMR (CDCl<sub>3</sub>, 500 MHz):  $\delta$  7.25 (d, J = 7.5 Hz, 2H), 6.47 (d, J = 7.0 Hz, 2H), 4.41 (br, 1H), 4.22 (q, J = 6.5 Hz, 2H), 4.09 (br, 1H), 3.85 (s, 2H), 1.27 (t, J = 6.3 Hz, 3H).  $^{13}$ C NMR (CDCl3, 125 MHz): δ 170.8, 147.5, 134.2, 125.4, 113.3, 61.6, 45.2, 14.3. GC-MS m/z (% relative intensity): 211 (36.0), 128 (100.0), 136 (23.8), 109 (11.3).

Ethyl 2-((4-aminophenyl)thio)acetate (6c). This compound was synthesized according to a modification of a previously reported procedure (Scheme S5).21 A flame dried 25 mL 2-neck round bottom flask was charged with 4-aminothiophenol 6a (200 mg, 1.60 mmol, 1 equiv.) and anhydrous THF (10 mL) under argon. The solution was cooled to -30° C and sodium hydride (66 mg, 1.66 mmol, 1.04 equiv.) was added in portions. After the reaction mixture was allowed to reach 0  $^{\circ}$  C, it was cooled again to -30  $^{\circ}$  C for the addition of ethyl bromoacetate (264 mg, 1.58 mmol, 0.99 equiv.), and stirred overnight at room temperature. The solvent was removed under reduced pressure and the crude product taken up in EtOAc (20 mL) and water (20 mL). The aqueous layer was extracted with EtOAc (3 x 20 mL). The combined organic layers were washed with aq. saturated NaHCO3 (10 mL), brine (10 mL) and water (10 mL), dried over Na<sub>2</sub>SO<sub>4</sub> and concentrated under reduced pressure. Purification by column chromatography on silica gel (0-40% EtOAc/hexanes) afforded ethyl 2-((4-aminophenyl)thio)acetate (6c) as a yellow oil (268 mg, 1.26 mmol, 79% yield). R<sub>f</sub> = 0.54 (20% EtOAc/hexanes). 1H NMR (CDCl<sub>3</sub>, 500 MHz):  $\delta$ 7.29 (d, J = 6.5 Hz, 2H), 6.60 (d, J = 7.0 Hz, 2H), 4.13 (t, J = 6.7)Hz, 2H), 3.76 (br, 2H), 3.45 (s, 2H), 1.21 (t, J = 6.5 Hz, 3H). <sup>13</sup>C NMR (CDCl3, 125 MHz): δ 170.3, 147.0, 135.0, 121.8, 115.6, 61.4, 39.3, 14.2. GC-MS m/z (% relative intensity): 211 (84.2), 212.1 (10.9), 138 (25.8), 124 (100.0).

### **ASSOCIATED CONTENT**

**Supporting Information**. Additional experimental data, synthetic schemes, and NMR spectra for all new compounds.

### **AUTHOR INFORMATION**

### **Corresponding Author**

\* rfasan@ur.rochester.edu

### **Author Contributions**

‡ E.J.M. and V.S. contributed equally to this work.

#### Notes

The authors declare no competing financial interest.

### **ACKNOWLEDGMENT**

This work was supported in part by the U.S. National Science Foundation (NSF) grant CHE-1609550 and in part by the U.S. National Institute of Health (NIH) grant GM098628. E.J.M. acknowledges support from the NIH Graduate Training Grant T32GM118283. MS instrumentation was supported by the U.S. NSF grant CHE-0946653. The authors are grateful to Dr. Jermaine Jenkins and the Structure Biology & Biophysics Facility at the University of Rochester for providing access to the CD instrumentation.

### **REFERENCES**

(1) (a) Miller, D. J.; Moody, C. J. Synthetic Applications of the O-H Insertion Reactions of Carbenes and Carbenoids Derived from Diazocarbonyl and Related Diazo-Compounds. *Tetrahedron* **1995**, *51*, 10811-10843; (b) Doyle, M. P.; Forbes, D. C. Recent Advances in Asymmetric Catalytic Metal Carbene Transformations. *Chem. Rev.* **1998**, *98*, 911-936; (c) Lebel, H.; Marcoux, J. F.; Molinaro, C.;

- Charette, A. B. Stereoselective Cyclopropanation Reactions. *Chem. Rev.* **2003**, *103*, 977-1050; (d) Zhang, Z. H.; Wang, J. B. Recent Studies on the Reactions of Alpha-Diazocarbonyl Compounds. *Tetrahedron* **2008**, *64*, 6577-6605; (e) Davies, H. M. L.; Morton, D. Guiding Principles for Site Selective and Stereoselective Intermolecular C-H Functionalization by Donor/Acceptor Rhodium Carbenes. *Chem. Soc. Rev.* **2011**, *40*, 1857-1869; (f) Zhu, S. F.; Zhou, Q. L. Transition-Metal-Catalyzed Enantioselective Heteroatom-Hydrogen Bond Insertion Reactions. *Acc. Chem. Res.* **2012**, *45*, 1365-1377.
- (2) (a) Bordeaux, M.; Tyagi, V.; Fasan, R. Highly Diastereoselective and Enantioselective Olefin Cyclopropanation Using Engineered Myoglobin-Based Catalysts. *Angew. Chem. Int. Ed.* **2015**, *54*, 1744–1748; (b) Bajaj, P.; Sreenilayam, G.; Tyagi, V.; Fasan, R. Gram-Scale Synthesis of Chiral Cyclopropane-Containing Drugs and Drug Precursors with Engineered Myoglobin Catalysts Featuring Complementary Stereoselectivity. *Angew. Chem. Int. Ed.* **2016**, *55*, 16110–16114; (c) Sreenilayam, G.; Moore, E. J.; Steck, V.; Fasan, R. Metal Substitution Modulates the Reactivity and Extends the Reaction Scope of Myoglobin Carbene Transfer Catalysts. *Adv. Synth. Cat.* **2017**, *359*, 2076–2089; (d) Tinoco, A.; Steck, V.; Tyagi, V.; Fasan, R. Highly Diastereo- and Enantioselective Synthesis of Trifluoromethyl-Substituted Cyclopropanes Via Myoglobin-Catalyzed Transfer of Trifluoromethylcarbene. *J. Am. Chem. Soc.* **2017**, *139*, 5293-5296.
- (3) (a) Coelho, P. S.; Brustad, E. M.; Kannan, A.; Arnold, F. H. Olefin Cyclopropanation Via Carbene Transfer Catalyzed by Engineered Cytochrome P450 Enzymes. *Science* **2013**, *339*, 307-310; (b) Coelho, P. S.; Wang, Z. J.; Ener, M. E.; Baril, S. A.; Kannan, A.; Arnold, F. H.; Brustad, E. M. A Serine-Substituted P450 Catalyzes Highly Efficient Carbene Transfer to Olefins in Vivo. *Nat. Chem. Biol.* **2013**, *9*, 485-487; (c) Gober, J. G.; Rydeen, A. E.; Gibson-O'Grady, E. J.; Leuthaeuser, J. B.; Fetrow, J. S.; Brustad, E. M. Mutating a Highly Conserved Residue in Diverse Cytochrome P450s Facilitates Diastereoselective Olefin Cyclopropanation. *Chembiochem* **2016**, *17*, 394-397; (d) Gober, J. G.; Ghodge, S. V.; Bogart, J. W.; Wever, W. J.; Watkins, R. R.; Brustad, E. M.; Bowers, A. A. P450-Mediated Non-Natural Cyclopropanation of Dehydroalanine-Containing Thiopeptides. *ACS Chem. Biol.* **2017**, *2*, 1726–1731.
- (4) (a) Wang, Z. J.; Peck, N. E.; Renata, H.; Arnold, F. H. Cytochrome P450-Catalyzed Insertion of Carbenoids into N-H Bonds. *Chem. Sci.* **2014**, *5*, 598-601; (b) Sreenilayam, G.; Fasan, R. Myoglobin-Catalyzed Intermolecular Carbene N-H Insertion with Arylamine Substrates. *Chem. Commun.* **2015**, *51*, 1532-1534.
- (5) Tyagi, V.; Bonn, R. B.; Fasan, R. Intermolecular Carbene S-H Insertion Catalysed by Engineered Myoglobin-Based Catalysts. *Chem. Sci.* **2015**, *6*, 2488-2494.
- (6) Kan, S. B. J.; Lewis, R. D.; Chen, K.; Arnold, F. H. Directed Evolution of Cytochrome C for Carbon-Silicon Bond Formation: Bringing Silicon to Life. *Science* **2016**, *354*, 1048-1051.
- (7) (a) Sreenilayam, G.; Moore, E. J.; Steck, V.; Fasan, R. Stereoselective Olefin Cyclopropanation under Aerobic Conditions with an Artificial Enzyme Incorporating an Iron-Chlorin E6 Cofactor. ACS Catal. 2017, 7, 7629-7633; (b) Key, H. M.; Dydio, P.; Clark, D. S.; Hartwig, J. F. Abiological Catalysis by Artificial Haem Proteins Containing Noble Metals in Place of Iron. Nature 2016, 534, 534-537; (c) Reynolds, E. W.; McHenry, M. W.; Cannac, F.; Gober, J. G.; Snow, C. D.; Brustad, E. M. An Evolved Orthogonal Enzyme/Cofactor Pair. J. Am. Chem. Soc. 2016, 138, 12451-12458; (d) Reynolds, E. W.; Schwochert, T. D.; McHenry, M. W.; Watters, J. W.; Brustad, E. M. Orthogonal Expression of an Artificial Metalloenzyme for Abiotic Catalysis. Chembiochem 2017, 18, 2380-2384; (e) Wolf, M. W.; Vargas, D. A.; Lehnert, N. Engineering of Rumb: Toward a Green Catalyst for Carbene Insertion Reactions. Inorg. Chem. 2017, 56, 5623-5635; (f) Ohora, K.; Meichin, H.; Zhao, L. M.; Wolf, M. W.; Nakayama, A.; Hasegawa, J.; Lehnert, N.; Hayashi, T. Catalytic Cyclopropanation by Myoglobin Reconstituted with Iron Porphycene: Acceleration of Catalysis Due to Rapid Formation of the Carbene Species. J. Am. Chem. Soc. 2017, 139, 17265-17268.

- (8) (a) Srivastava, P.; Yang, H.; Ellis-Guardiola, K.; Lewis, J. C. Engineering a Dirhodium Artificial Metalloenzyme for Selective Olefin Cyclopropanation. *Nat. Commun.* **2015**, *6*, 7789; (b) Rioz-Martinez, A.; Oelerich, J.; Segaud, N.; Roelfes, G. DNA-Accelerated Catalysis of Carbene-Transfer Reactions by a DNA/Cationic Iron Porphyrin Hybrid. *Angew. Chem. Int. Ed.* **2016**, *55*, 14136-14140.
- (9) Talele, T. T. The "Cyclopropyl Fragment" Is a Versatile Player That Frequently Appears in Preclinical/Clinical Drug Molecules. *J. Med. Chem.* **2016**, *59*, 8712-8756.
- (10) (a) Galardon, E.; Le Maux, P.; Simonneaux, G. Cyclopropanation of Alkenes, N-H and S-H Insertion of Ethyl Diazoacetate Catalysed by Ruthenium Porphyrin Complexes. *Tetrahedron* **2000**, *56*, 615-621; (b) Aviv, I.; Gross, Z. Iron Corroles and Porphyrins as Very Efficient and Highly Selective Catalysts for the Reactions of Alpha-Diazo Esters with Amines. *Synlett* **2006**, 951-953; (c) Baumann, L. K.; Mbuvi, H. M.; Du, G.; Woo, L. K. Iron Porphyrin Catalyzed N-H Insertion Reactions with Ethyl Diazoacetate. *Organometallics* **2007**, *26*, 3995-4002; (d) Noels, A. F.; Demonceau, A.; Petiniot, N.; Hubert, A. J.; Teyssie, P. Transition-Metal-Catalyzed Reactions of Diazo-Compounds, Efficient Synthesis of Functionalized Ethers by Carbene Insertion into the Hydroxylic Bond of Alcohols. *Tetrahedron* **1982**, *38*, 2733-2739; (e) Zhu, S. F.; Cai, Y.; Mao, H. X.; Xie, J. H.; Zhou, Q. L. Enantioselective Iron-Catalysed O-H Bond Insertions. *Nat. Chem.* **2010**, *2*, 546-551.
- (11) (a) Bagheri, V.; Doyle, M. P.; Taunton, J.; Claxton, E. E. A New and General-Synthesis of Alpha-Silyl Carbonyl-Compounds by Si-H Insertion from Transition-Metal Catalyzed-Reactions of Diazo Esters and Diazo Ketones. *J. Org. Chem.* **1988**, *53*, 6158-6160; (b) Andrey, O.; Landais, Y.; Planchenault, D. A One-Pot Synthesis of Alpha-(Alkoxysilyl)Acetic Esters. *Tetrahedron Lett.* **1993**, *34*, 2927-2930; (c) Wang, J. C.; Xu, Z. J.; Guo, Z.; Deng, Q. H.; Zhou, C. Y.; Wan, X. L.; Che, C. M. Highly Enantioselective Intermolecular Carbene Insertion to C-H and Si-H Bonds Catalyzed by a Chiral Iridium(Iii) Complex of a D-4-Symmetric Halterman Porphyrin Ligand. *Chem. Commun.* **2012**, *48*, 4299-4301; (d) Keipour, H.; Ollevier, T. Iron-Catalyzed Carbene Insertion Reactions of Alpha-Diazoesters into Si-H Bonds. *Organic Letters* **2017**, *19*, 5736-5739.
- (12) (a) Sambasivan, R.; Ball, Z. T. Metallopeptides for Asymmetric Dirhodium Catalysis. *J. Am. Chem. Soc.* **2010**, *132*, 9289-9291; (b) Yang, H.; Srivastava, P.; Zhang, C.; Lewis, J. C. A General Method for Artificial Metalloenzyme Formation through Strain-Promoted Azide-Alkyne Cycloaddition. *Chembiochem* **2014**, *15*, 223-227.
- (13) Zhang, K. D.; El Damaty, S.; Fasan, R. P450 Fingerprinting Method for Rapid Discovery of Terpene Hydroxylating P450 Catalysts with Diversified Regioselectivity. *J. Am. Chem. Soc.* **2011**, 133, 3242-3245.
- (14) Wei, Y.; Tinoco, A.; Steck, V.; Fasan, R.; Zhang, Y. Cyclopropanations Via Heme Carbenes: Basic Mechanism and Effects of Carbene Substituent, Protein Axial Ligand, and Porphyrin Substitution. *J. Am. Chem. Soc.* **2018**, *140*, 1649-1662.
- (15) Vojtechovsky, J.; Chu, K.; Berendzen, J.; Sweet, R. M.; Schlichting, I. Crystal Structures of Myoglobin-Ligand Complexes at near-Atomic Resolution. *Biophys. J.* **1999**, *77*, 2153-2174.
- (16) Bordeaux, M.; Singh, R.; Fasan, R. Intramolecular C(Sp(3))H Amination of Arylsulfonyl Azides with Engineered and Artificial Myoglobin-Based Catalysts. *Bioorg. Med. Chem.* **2014**, *22*, 5697-5704.
- (17) Kunze, C.; Bommer, M.; Hagen, W. R.; Uksa, M.; Dobbek, H.; Schubert, T.; Diekert, G. Cobamide-Mediated Enzymatic Reductive Dehalogenation Via Long-Range Electron Transfer. *Nat. Commun.* **2017**, *8*, ARTN 15858.
- (18) Moore, E. J.; Zorine, D.; Hansen, W. A.; Khare, S. D.; Fasan, R. Enzyme Stabilization Via Computationally Guided Protein Stapling. *Proc. Natl. Acad. Sci. USA* **2017**, *114*, 12472-12477.
- (19) Aller, E.; Brown, D. S.; Cox, G. G.; Miller, D. J.; Moody, C. J. Diastereoselectivity in the O-H Insertion Reactions of Rhodium Carbenoids Derived from Phenyldiazoacetates of Chiral Alcohols -

Preparation of Alpha-Hydroxy and Alpha-Alkoxy Esters. *J. Org. Chem.* **1995**, *60*, 4449-4460.

- (20) Bettanin, L.; Saba, S.; Galetto, F. Z.; Mike, G. A.; Rafique, J.; Braga, A. L. Solvent- and Metal-Free Selective Oxidation of Thiols to Disulfides Using I-2/Dmso Catalytic System. *Tetrahedron Lett.* **2017**, *58*, 4713-4716.
- (21) Chen, B. B.; Chen, H. Y.; Gesicki, G. J. In *Pat. Appl. EP0891325-B1*; GD Searle LLC: 1996.

# Supporting Information for

# Chemoselective Cyclopropanation over Carbene Y—H insertion Catalyzed by an Engineered Carbene Transferase

Eric J. Moore<sup>‡</sup>, Viktoria Steck<sup>‡</sup>, Priyanka Bajaj, and Rudi Fasan\*

Department of Chemistry, University of Rochester, 14627 Rochester, New York, USA

Correspondence should be addressed to R.F. (rfasan@ur.rochester.edu)

### **Table of contents:**

Supplementary Schemes S1-S5 Pages S1-S3

NMR spectra Pages S4-S18

# Scheme S1. Activity and selectivity for Mb(H64V,V68A)[Co(ppIX)]-catalyzed cyclopropanation of selected vinylarenes with EDA.<sup>a</sup>

### Scheme S2. Synthetic route for the preparation of compound 4b.

### Scheme S3. Synthetic route for the preparation of compound 5c.

<sup>&</sup>lt;sup>a</sup> Reaction conditions: 10 mM olefin, 20 mM EDA, *E. coli* whole cells expressing Mb(H64V,V68A)[(Co(ppIX)] (OD<sub>600</sub> = 80) in 50 mM phosphate buffer (pH 7.2). <sup>b</sup> Based on GC conversion. <sup>c</sup> For *trans*-(1*S*,2*S*) product.

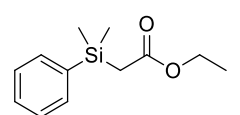
# Scheme S4. Synthetic route for the preparation of compound 6b.

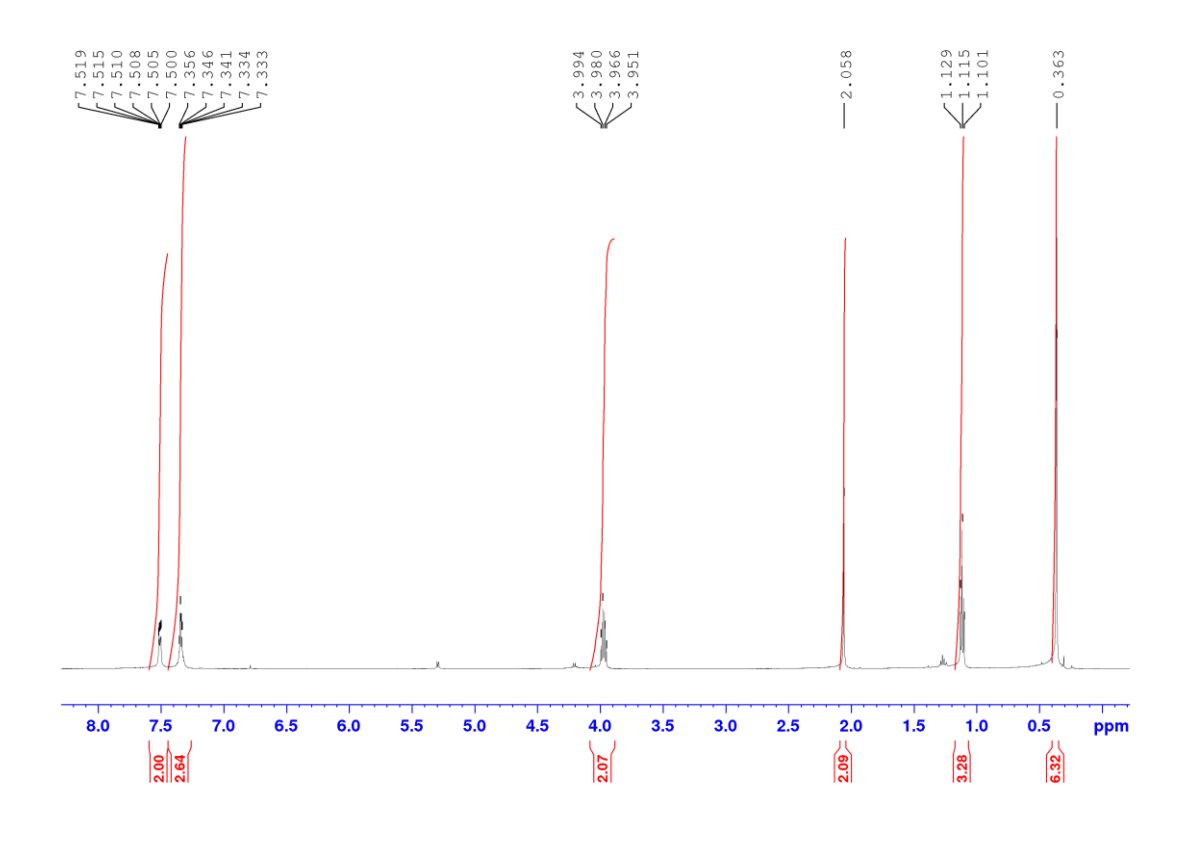
SH 
$$I_2$$
  $I_2$   $I_3$   $I_4$   $I_4$   $I_5$   $I$ 

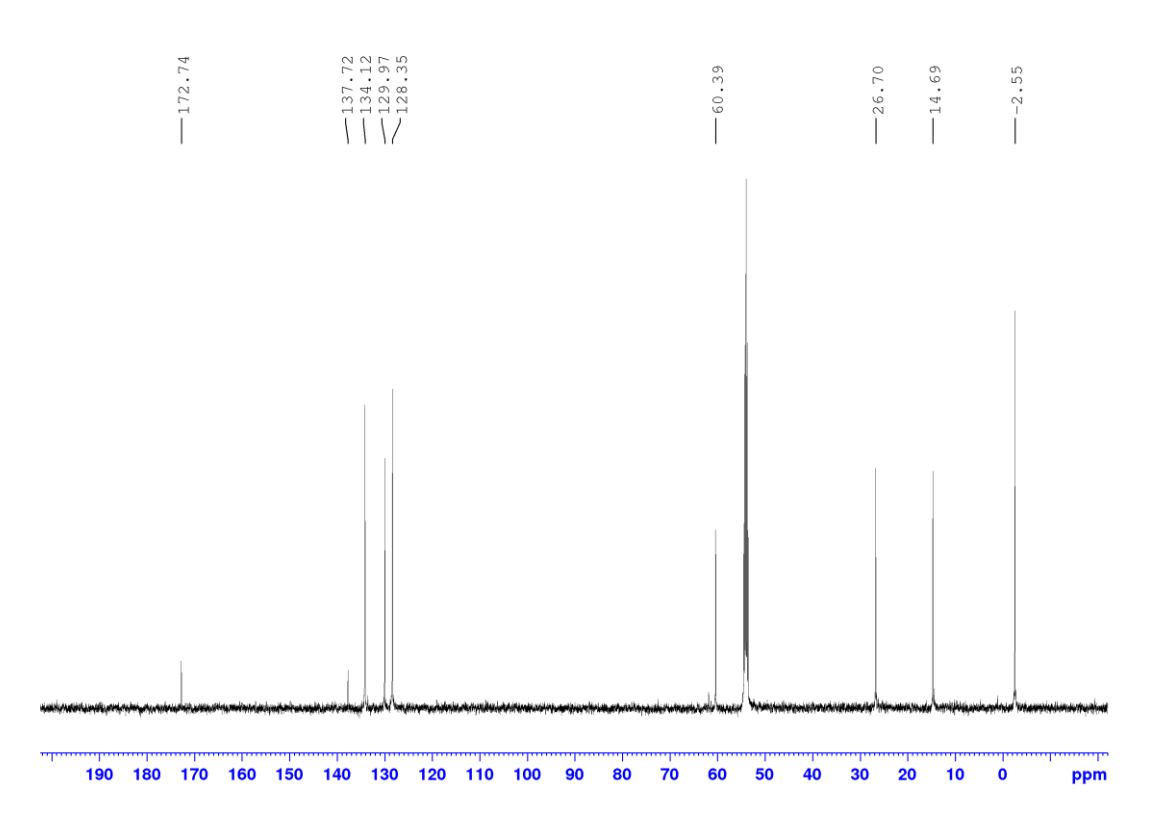
# Scheme S5. Synthetic route for the preparation of compound 6c.

# **NMR Spectra**

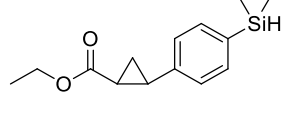
Ethyl 2-(dimethyl(phenyl)silyl)acetate 1b.



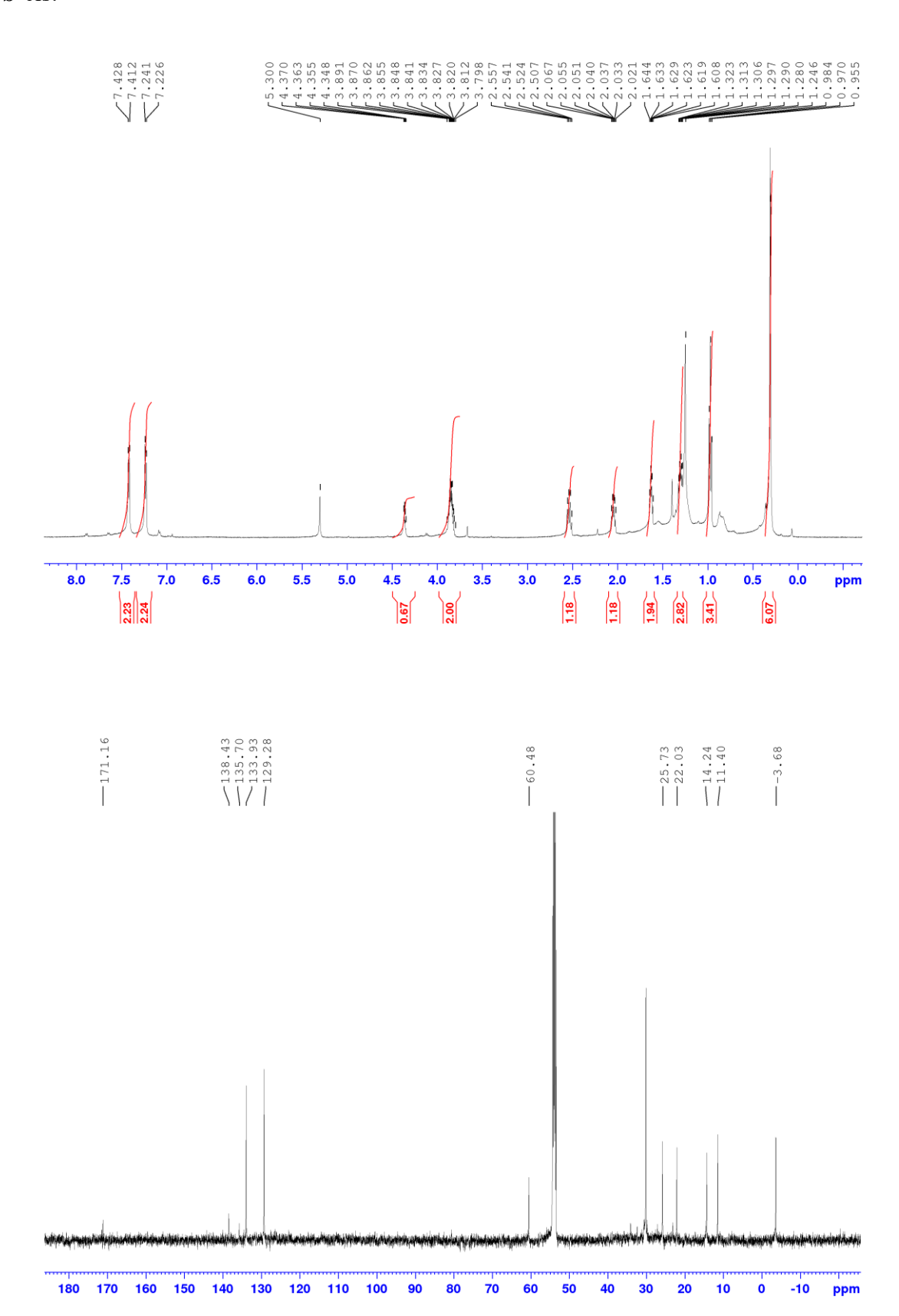




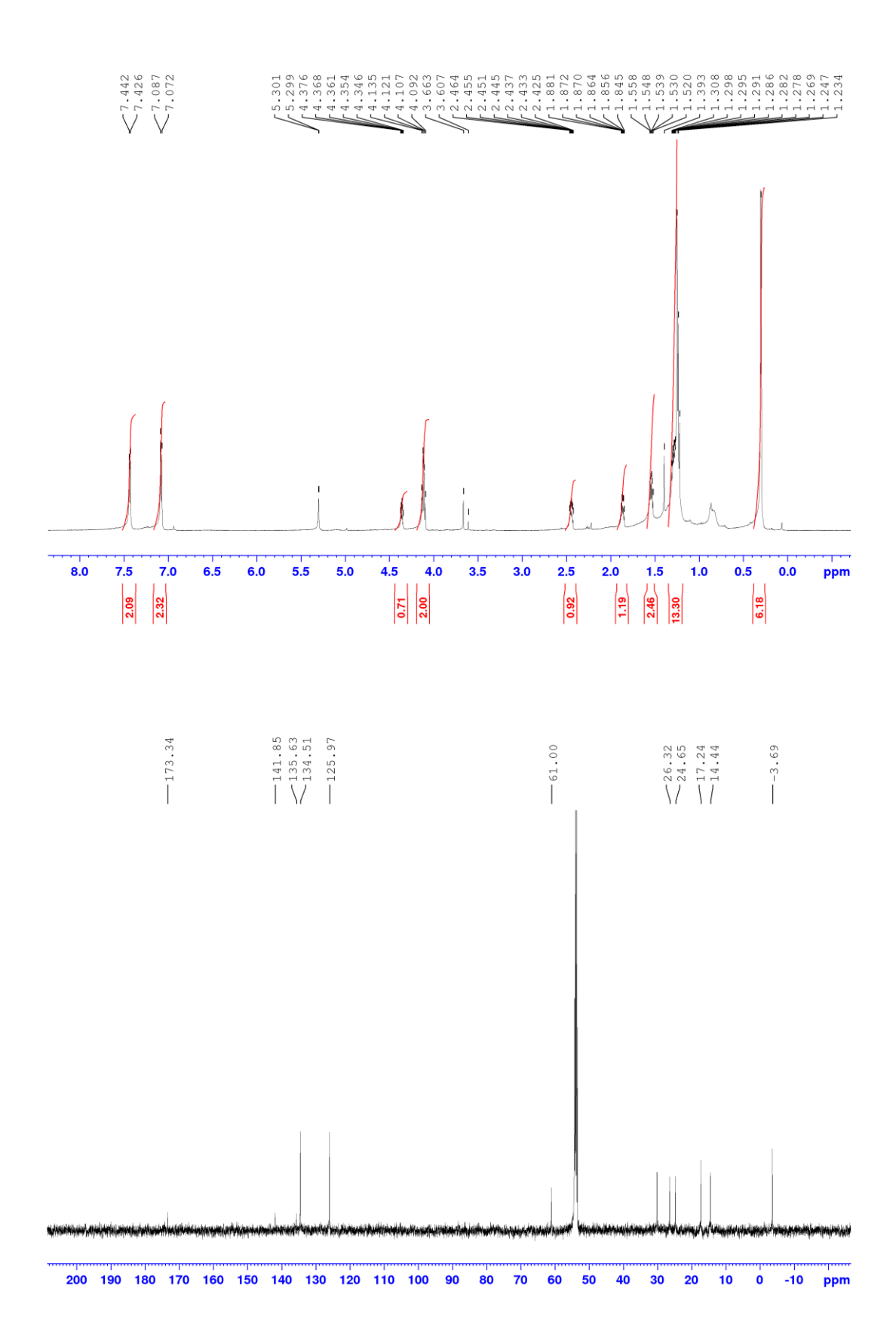
Ethyl 2-(4-(dimethylsilyl)phenyl)cyclopropanecarboxylate **3b**.

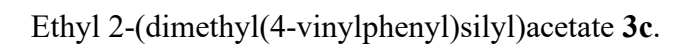


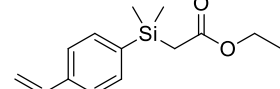
### 3b-cis:

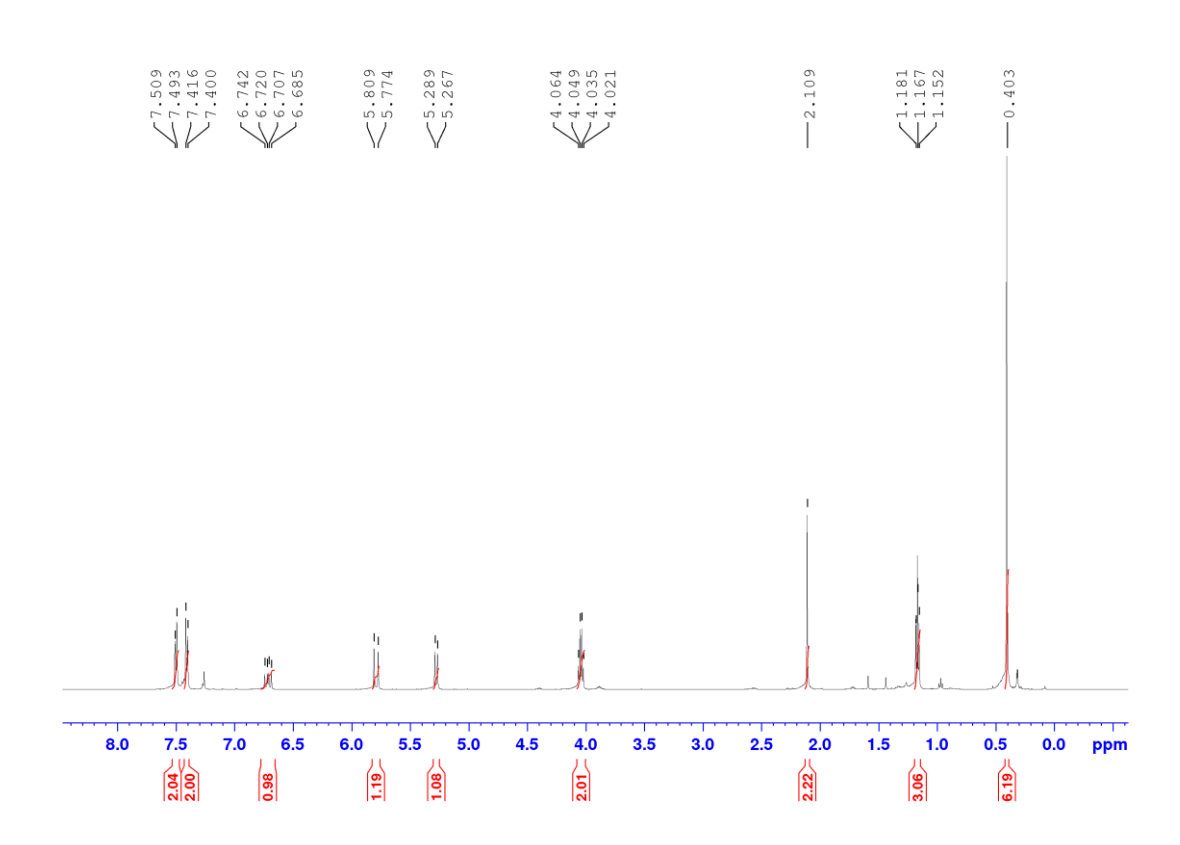


### **3b**-trans:

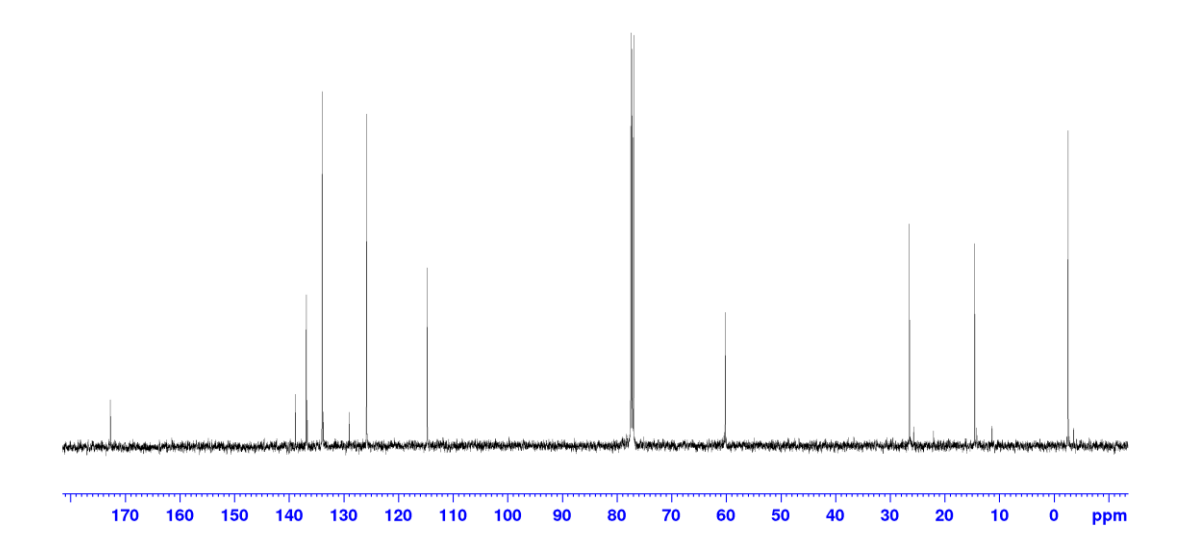


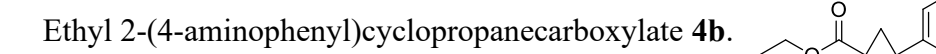




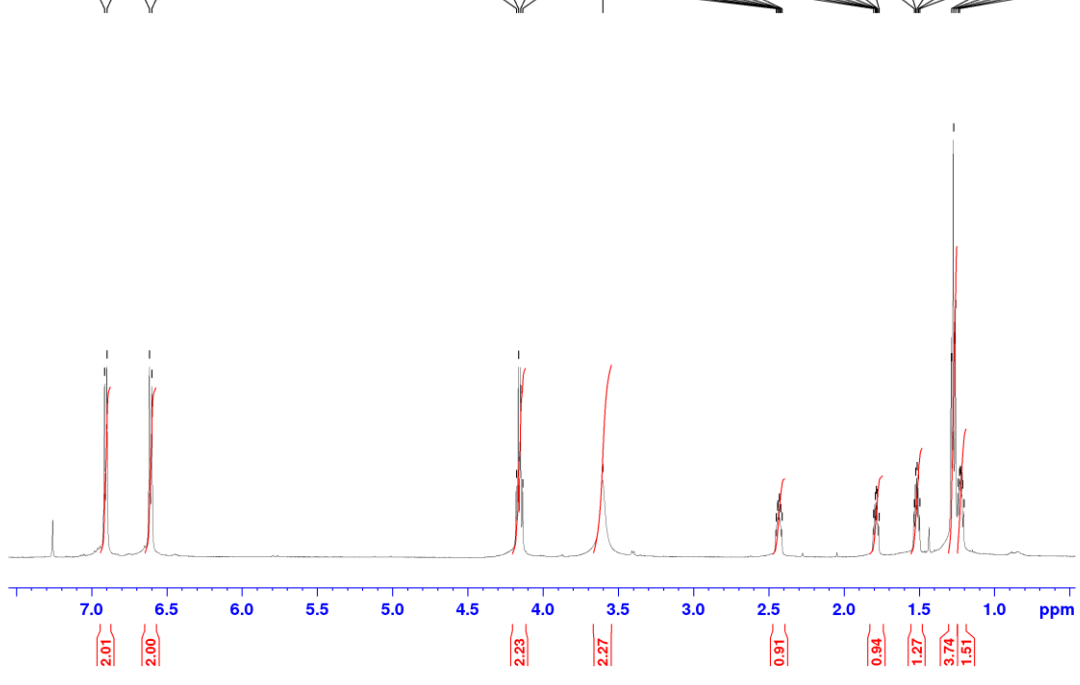


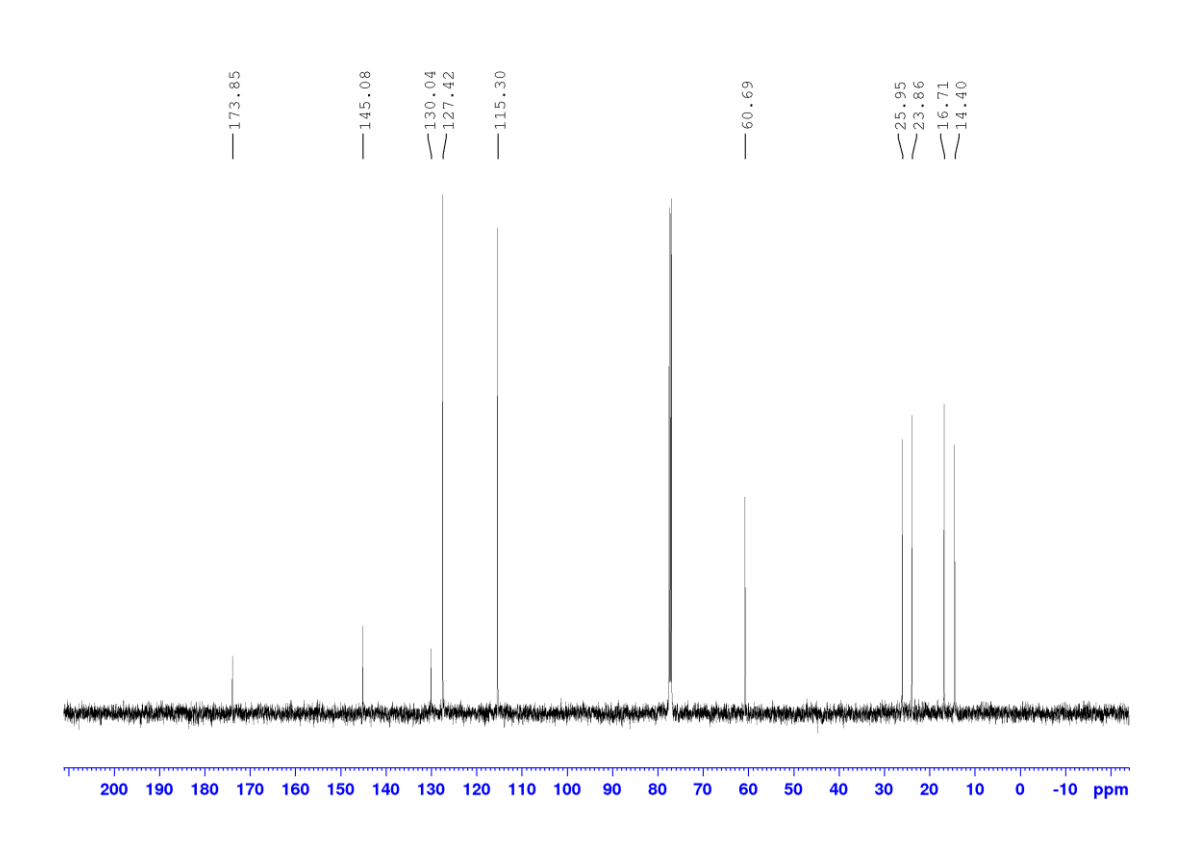






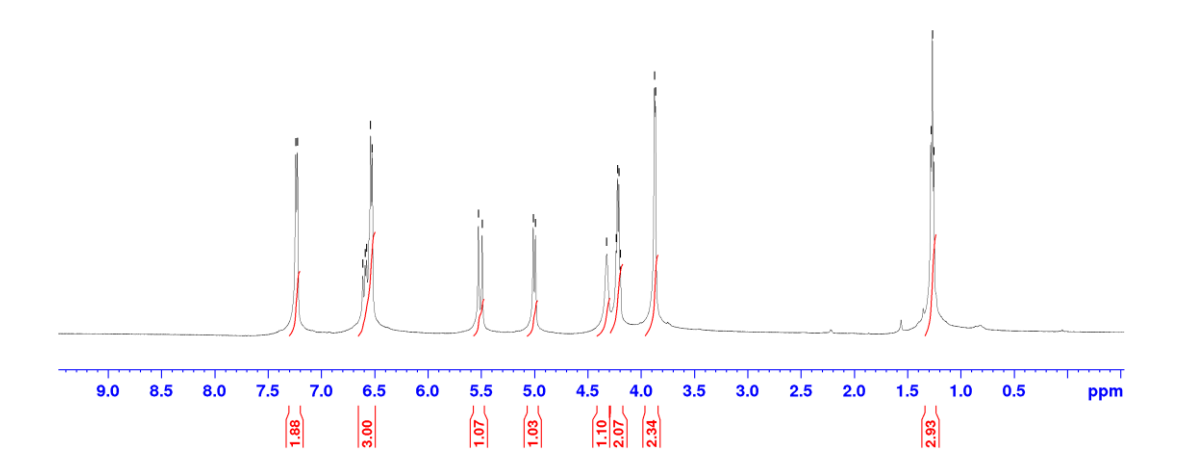


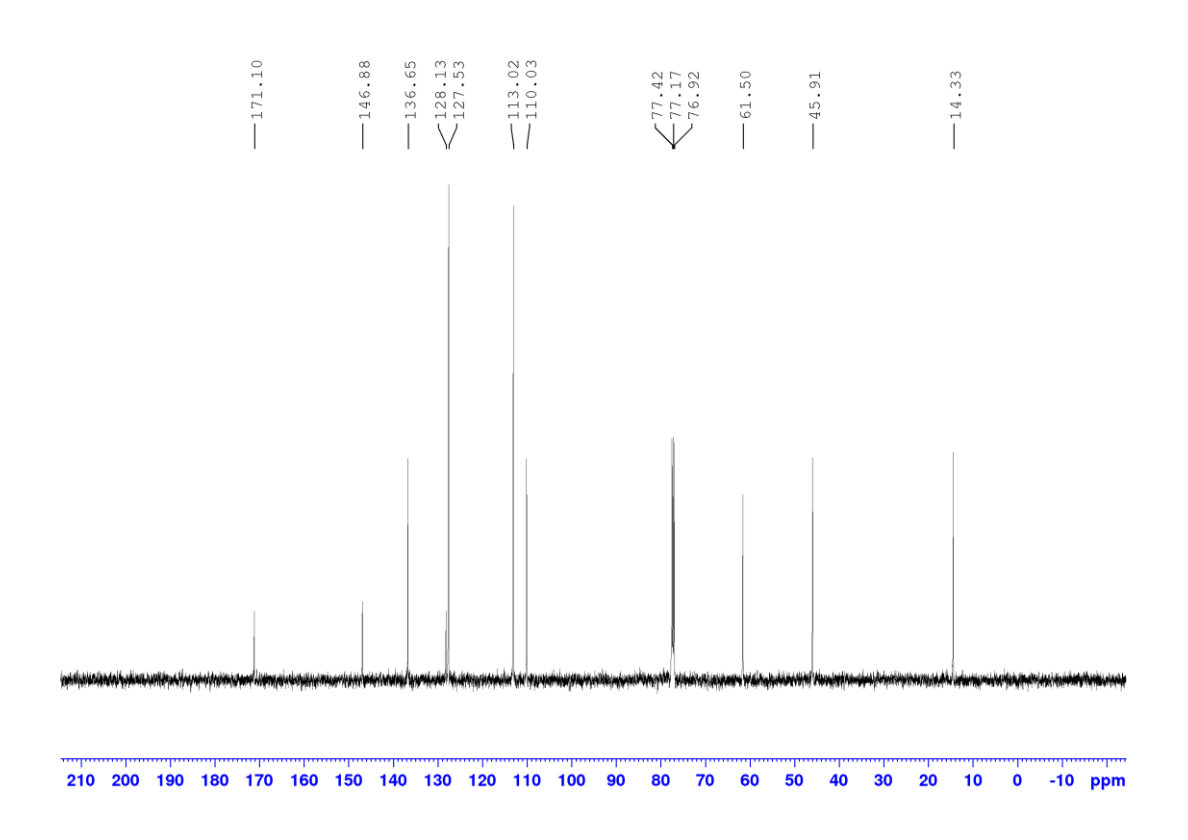


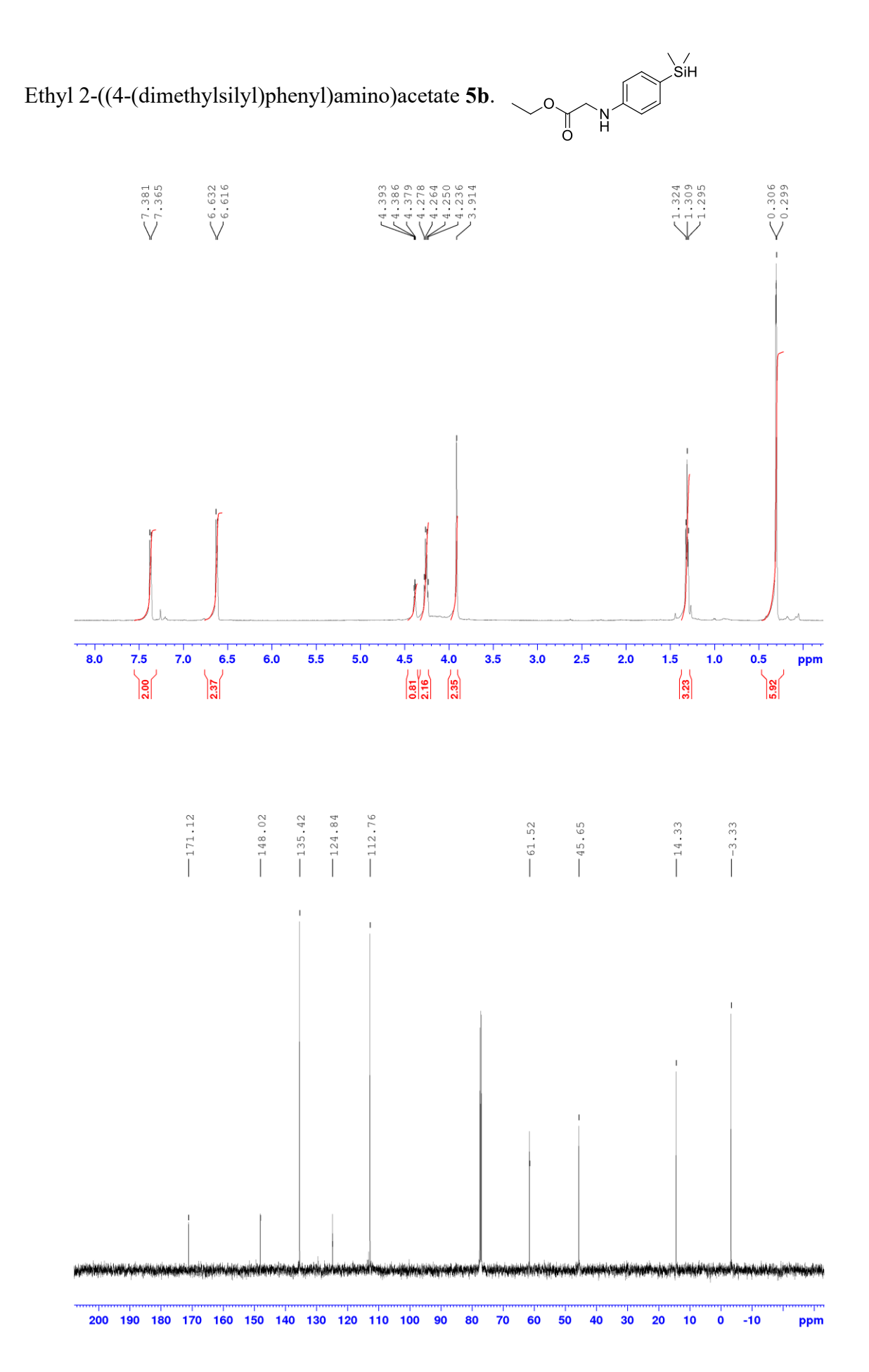


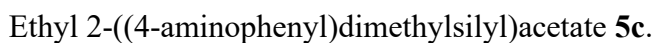
Ethyl 2-((4-vinylphenyl)amino)acetate **4c**.

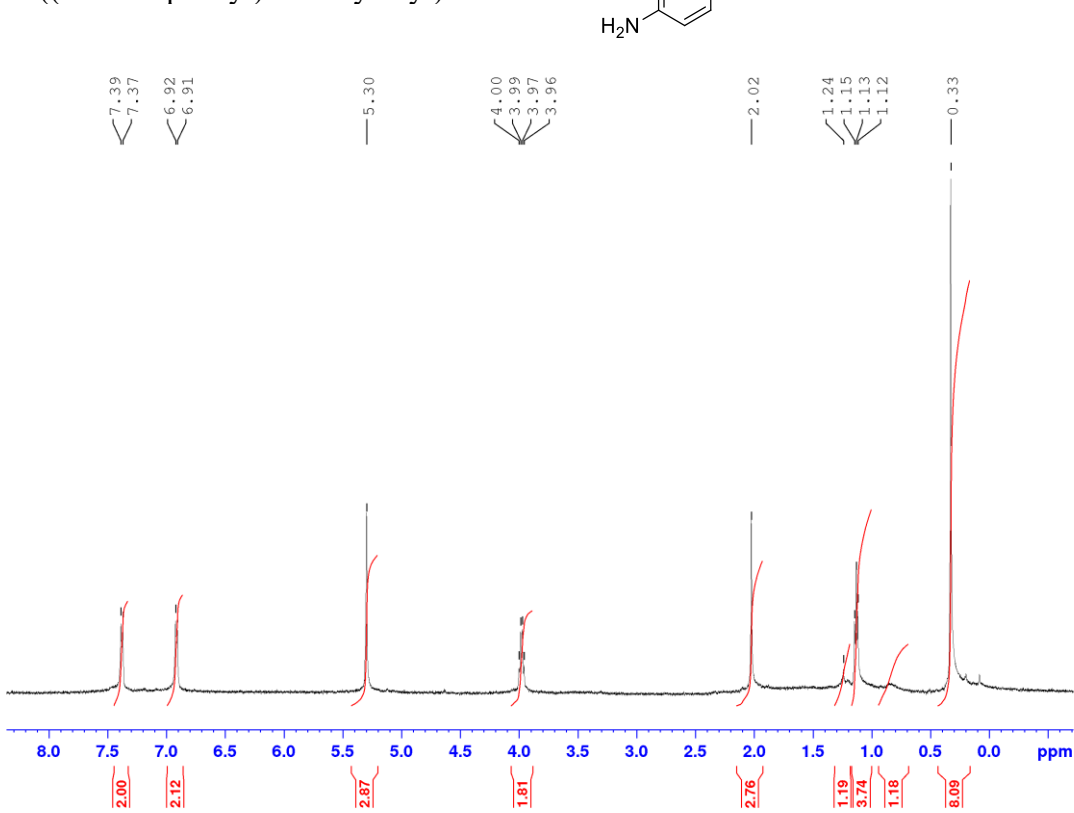




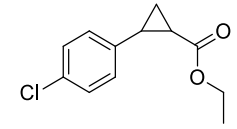




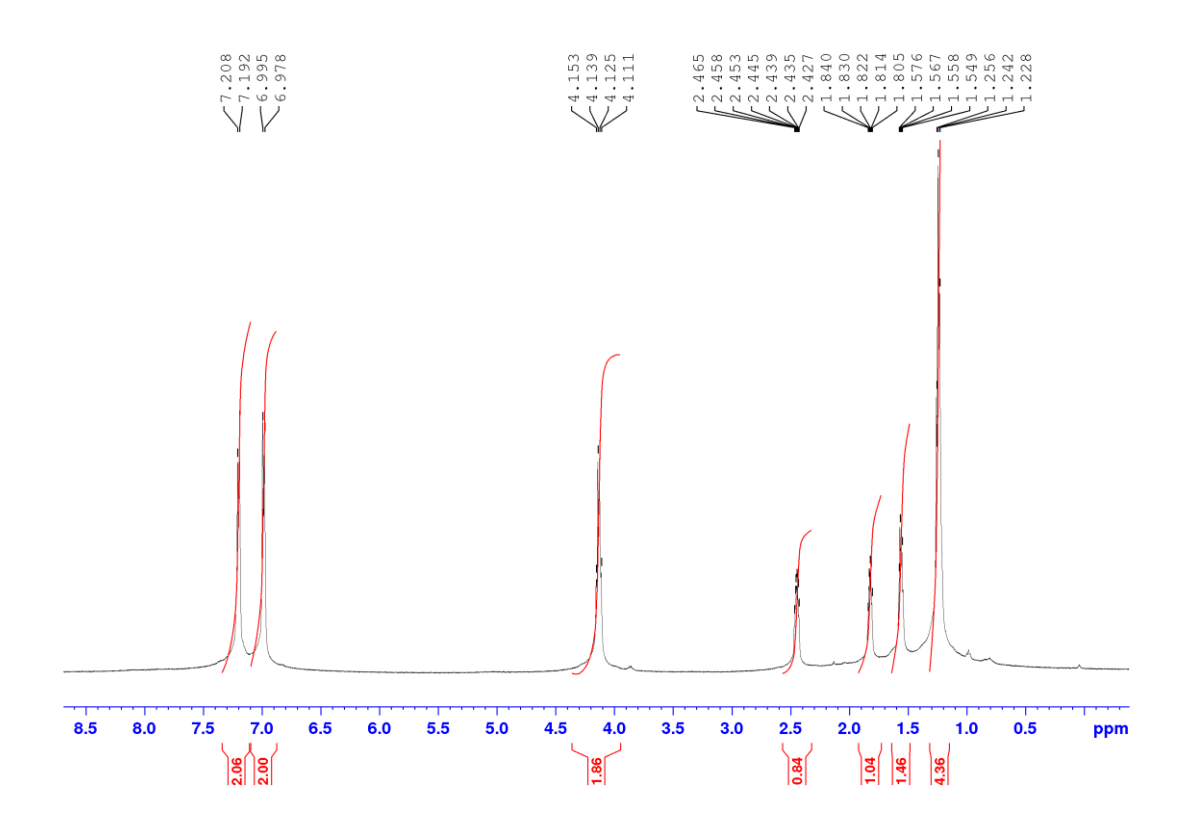




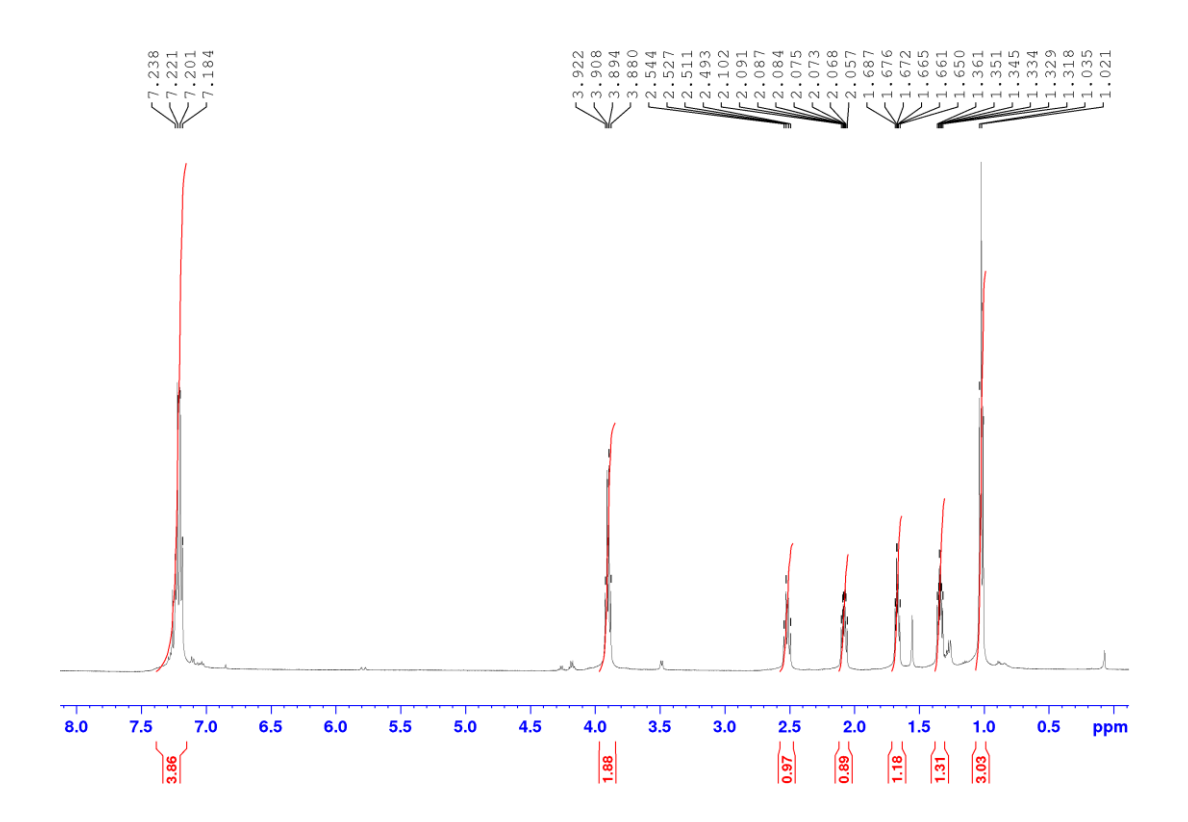
Ethyl 2-(4-chlorophenyl)cyclopropanecarboxylate 10b.

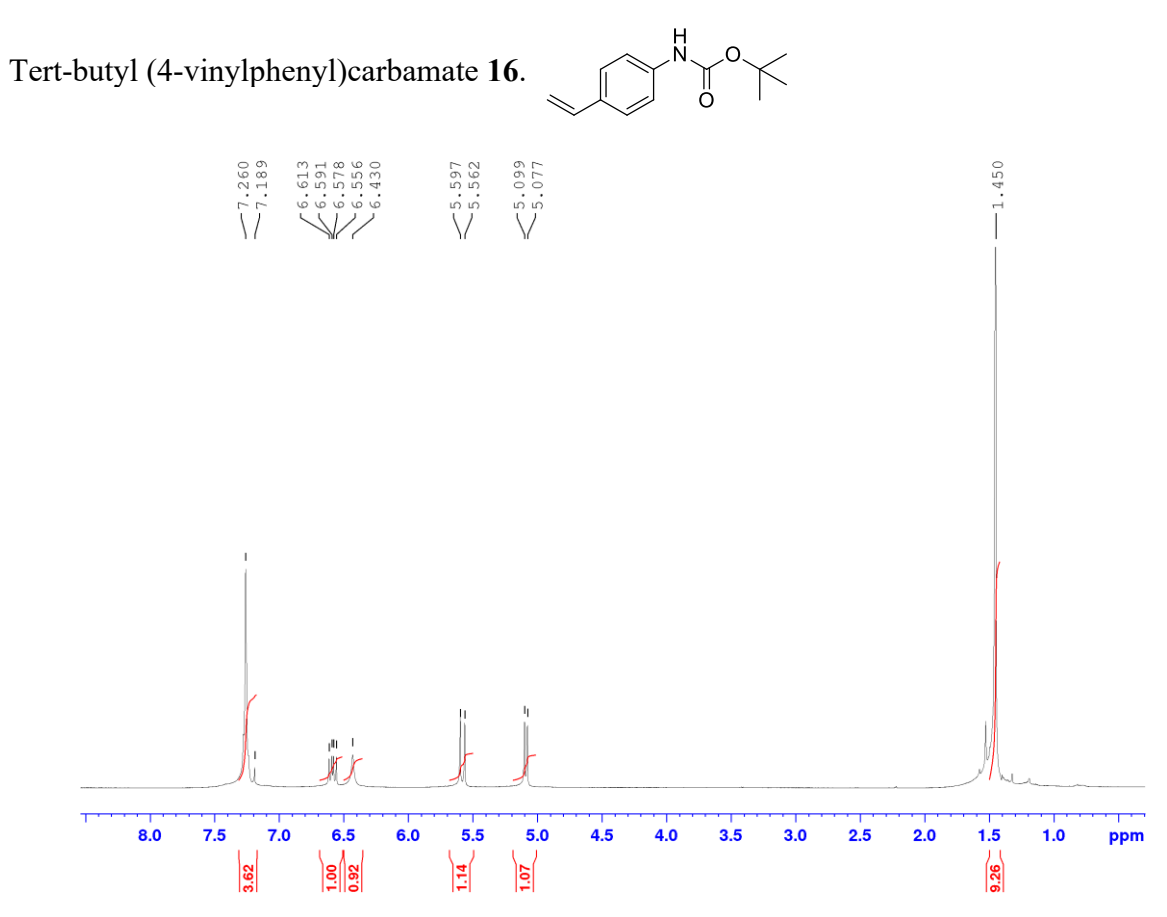


# 10b-trans:

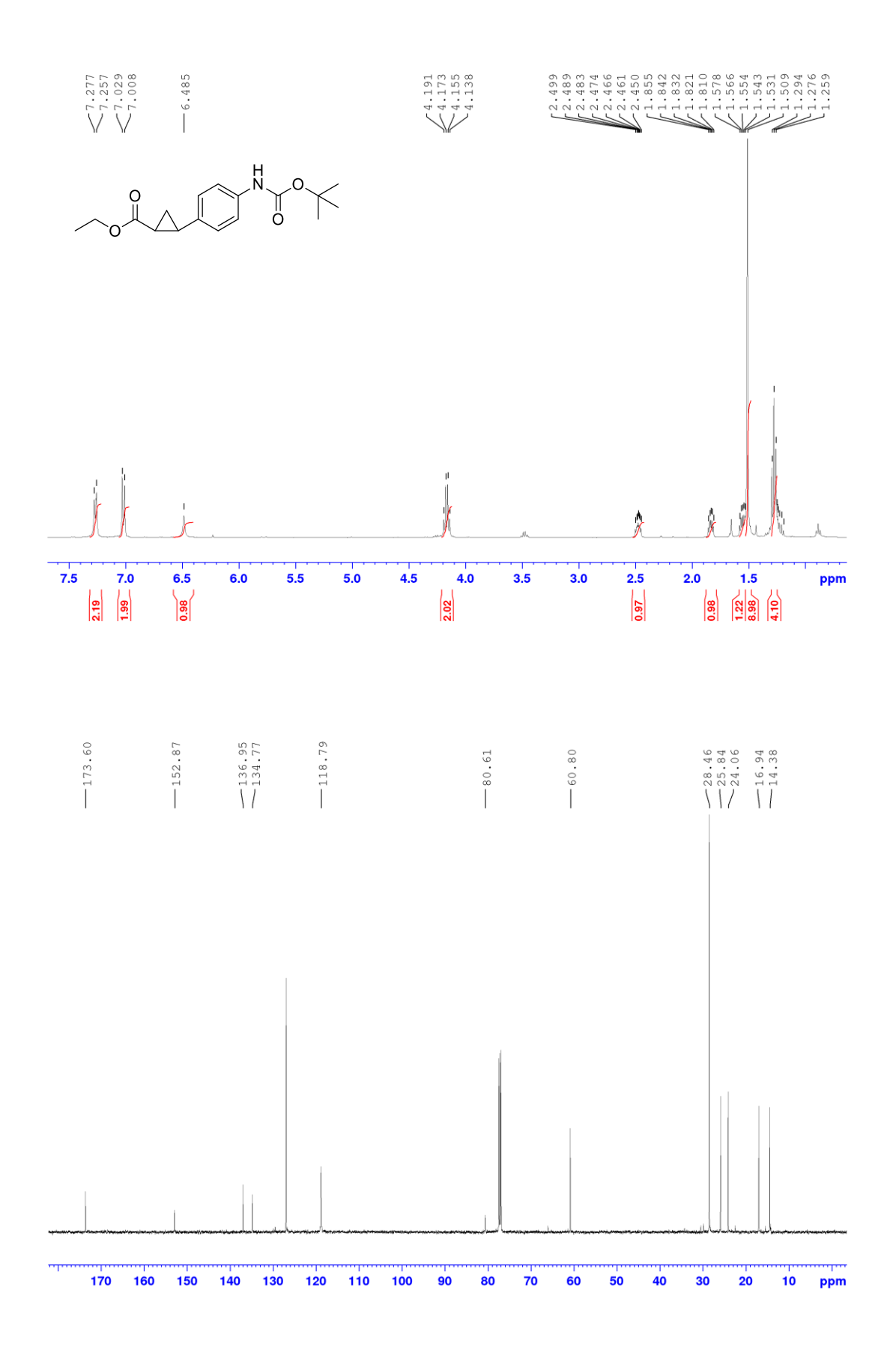


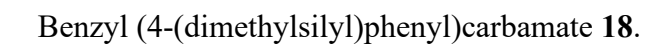
## **10b-cis**:

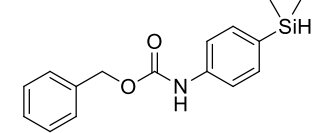


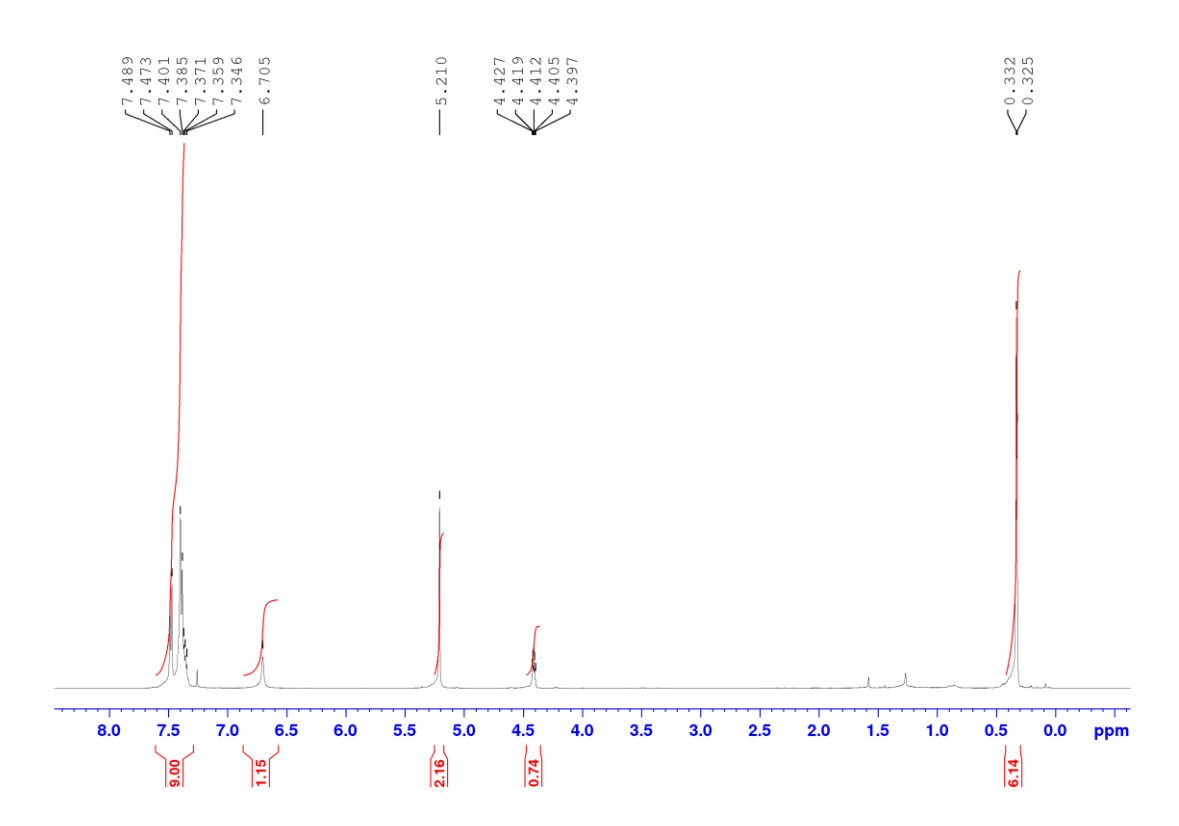


Ethyl 2-(4-((tert-butoxycarbonyl)amino)phenyl)cyclopropanecarboxylate 17.

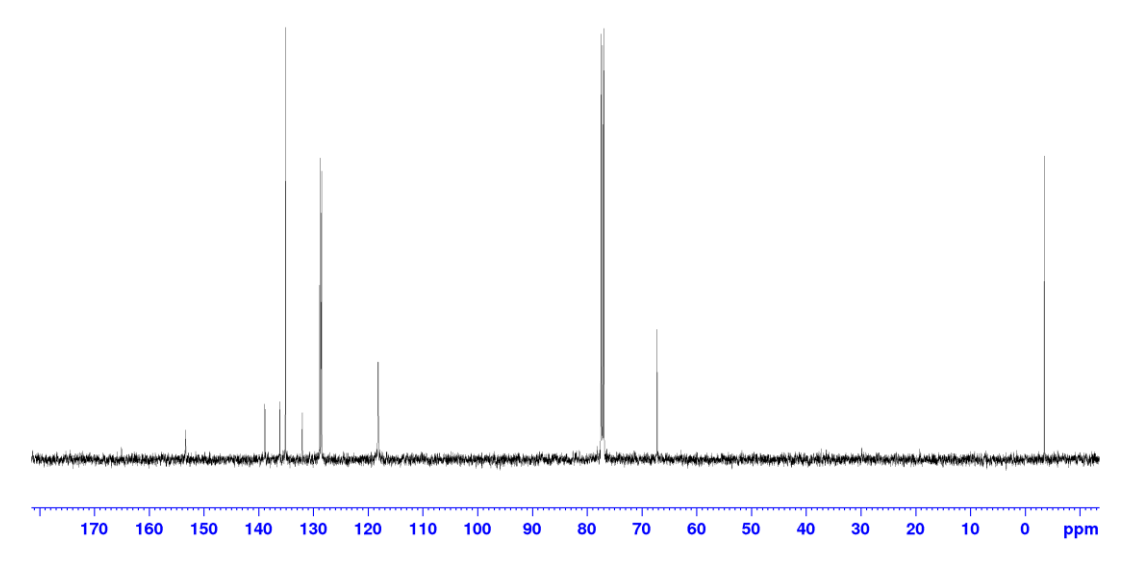












Ethyl 2-((4-(((benzyloxy)carbonyl)amino)phenyl)dimethylsilyl)acetate 19.

